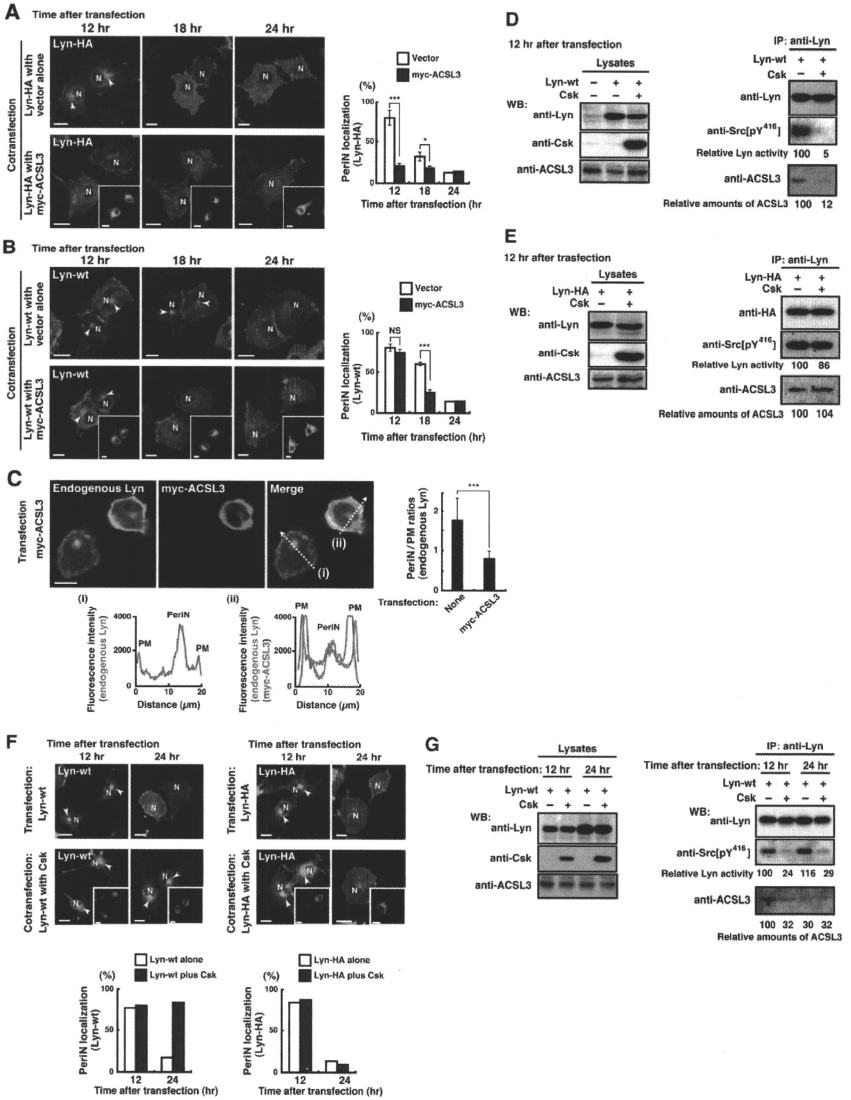

Fig. 2. See next page for legend.

Fig. 2. Effect of ACSL3 overexpression on Lyn trafficking. (**A**,**B**) COS-1 cells transfected with (A) Lyn-HA in conjunction with vector alone or Myc-ACSL3 or (B) Lyn-wt in conjunction with vector alone or Myc-ACSL3 were cultured for the indicated times. Cells were doubly stained with anti-HA (red) and anti-Myc (green) antibodies (A) or anti-Lyn (red) and anti-Myc (green) antibodies (B). Insets show fluorescence images of Myc-ACSL3. Arrowheads indicate the perinuclear region. N, nucleus. Scale bars: 20 μm. Cells exhibiting predominant perinuclear localization of Lyn-HA (A) and Lyn-wt (B) were quantified, and results (%) represent means ± s.d. from three independent experiments (n>200). Asterisks indicate significant differences (*P<0.05; ***P<0.001; NS, not significant) calculated by Student's t-test. The results 24 hours after transfection are from a representative experiment (n>200). (**C**) THP-1 cells transfected with Myc-ACSL3 were cultured for 48 hours and doubly stained with anti-Lyn (green) and anti-Myc (red) antibodies. Intensity plots along the dotted lines (i, ii) are shown for endogenous Lyn (green line) and Myc-ACSL3 (red line). PeriN/PM ratios of endogenous Lyn indicate mean fluorescence intensity of endogenous Lyn localized to the PeriN relative to that localized to the PM. Results represent means ± s.d. from untransfected cells (n=27) and Myc-ACSL3-expressing cells (n=28). Asterisks indicate the significant difference (***P<0.001) calculated by Student's t-test. Scale bar: 10 μm. PeriN, perinuclear region; PM, plasma membrane. (**D**,**E**) COS-1 cells transfected with Lyn-wt (D) or Lyn-HA (E) were cultured for 12 hours. To achieve excessive overexpression of CSK, COS-1 cells transfected with excess CSK for 10 hours were subsequently cotransfected with Lyn-wt plus CSK (D) or Lyn-HA plus CSK (E) and cultured for further 12 hours. Lyn-wt and Lyn-HA were immunoprecipitated from Triton X-100 cell lysates with anti-Lyn antibody. Immunoblotting was performed for Lyn, HA, ACSL3, CSK and phosphorylated Src (pY^{416}). Lyn activities and amounts of coimmunoprecipitated endogenous ACSL3 were normalized to the amounts of Lyn present in the immunoprecipitates. (**F**) COS-1 cells were transfected with Lyn-wt, Lyn-wt plus CSK, Lyn-HA, or Lyn-HA plus CSK were cultured for 12 hours, and excessive overexpression of CSK was performed as described above. Cells were doubly stained with anti-Lyn (green) and anti-CSK antibodies (red). Insets show fluorescence images of CSK. Arrowheads indicate the perinuclear region. N, nucleus. Scale bars: 20 μm. Cells exhibiting predominant perinuclear localization of Lyn-wt (left) and Lyn-HA (right) were quantified12 hours and 24 hours after transfection, and results were obtained from representative experiments (12 hours, n>200) and (24 hours, n>175). (**G**) Triton X-100 cell lysates prepared as described in F were used for immunoprecipitation with anti-Lyn antibody. Immunoblotting was performed for Lyn, ACSL3, CSK and phosphorylated Src. Lyn activities and amounts of coimmunoprecipitated endogenous ACSL3 were normalized to the amounts of Lyn present in the immunoprecipitates.

accumulated, despite colocalization of Myc-ACSL3 largely with ER-resident calnexin (supplementary material Fig. S2). We then transfected COS-1 cells with Lyn-wt to examine the localization of Lyn and ACSL3, because endogenous Lyn could not be visualized owing to its low expression in COS-1 cells. At 18 hours after transfection, Lyn-wt was localized to the Golgi and the plasma membrane. Endogenous ACSL3 was seen mainly at the perinuclear areas but not at the plasma membrane, consistent with previous studies (Fujimoto et al., 2004), and Lyn-wt was colocalized with endogenous ACSL3 at the Golgi, but not the plasma membrane (Fig. 1I, upper panels). In addition, Lyn-wt was colocalized with Myc-ACSL3 at the Golgi but not the plasma membrane in COS-1 cells cotransfected with Lyn-wt and Myc-ACSL3 (Fig. 1I, lower panels). Localization of Myc-ACSL3 was comparable with that of endogenous ACSL3 (Fig. 1G). These results suggest that Lyn is associated with ACSL3 at the Golgi.

Requirement of Lyn open conformation for its association with ACSL3

To examine the role of ACSL3 in Lyn localization, we overexpressed ACSL3 in COS-1 cells and found that coexpression of Myc-ACSL3 permitted Lyn-HA and Lyn-wt to localize to the plasma membrane at 12 hours and 18 hours after transfection, respectively (Fig. 2A,B). The trafficking of Lyn from the Golgi to the plasma membrane was accelerated by the lack of the C-terminal negative-regulatory tail in Lyn (compare Fig. 2A with 2B). Similar results were obtained in HeLa cells (supplementary material Fig. S3). By contrast, overexpression of ACSL3 did not affect the localization of Src, the Golgi pool of caveolin or Golgi-resident GM130 and GalT (supplementary material Fig. S4), suggesting that overexpression of ACSL3 specifically accelerates the trafficking of Lyn from the Golgi. Note that Myc-ACSL3 consistently remained in the perinuclear areas (insets in Fig. 2A,B; Fig. 3B). In human monocytic THP-1 cells, endogenous Lyn can be visualized at the Golgi and the plasma membrane (Ikeda et al., 2008; Sato et al., 2009). We found that expression of Myc-ACSL3 in THP-1 cells significantly decreased the levels of endogenous Lyn at the Golgi and increased its levels at the plasma membrane (Fig. 2C). Moreover, excessive overexpression of CSK greatly decreased the levels of the association of Lyn-wt with endogenous ACSL3 in COS-1 cells, leading to blockade of Golgi export of Lyn-wt even at 24 hours after transfection, whereas excessive overexpression of CSK did not inhibit Lyn-HA association with ACSL3 nor Golgi export of Lyn-HA (Fig. 2D-F). To further examine the relationship between the localization of Lyn and its association with ACSL3, we compared the association of Lyn with ACSL3 between 12 hours and 24 hours after transfection. The amount of ACSL3 that associated with Lyn-wt 24 hours after transfection was drastically decreased compared with the amount associated with CSK-treated Lyn-wt (Fig. 2G), suggesting that Lyn present at the plasma membrane was not colocalized with ACSL3 (see also Fig. 1I; Fig. 2A-C, Fig. 3B, Fig. 4C, Fig. 7C; supplementary material Fig. S3). These results suggest that Golgi association of Lyn in its open conformation with ACSL3 initiates and accelerates Golgi export of Lyn toward the plasma membrane.

Role of Lyn C-lobe charged residues in ACSL3 association in vivo

Next, we compared the effect of ACSL3 overexpression on the trafficking between Lyn-HA and Tetra-mt-HA, which lacks the four charged residues in the C-lobe (Fig. 1A). The levels of Tetra-mt-HA coimmunoprecipitated with Myc-ACSL3 were lower than those of Lyn-HA coimmunoprecipitated with Myc-ACSL3 (Fig. 3A). Tetra-mt-HA was predominantly seen at the Golgi in COS-1 cells transfected with Tetra-mt-HA alone at 11 hours and 12 hours after transfection (Fig. 3B, upper panels), consistent with our previous study (Kasahara et al., 2004). We further showed that in COS-1 cells coexpressing Tetra-mt-HA plus Myc-ACSL3 or Lyn-HA plus Myc-ACSL3, expression of Myc-ACSL3 did not accelerate Golgi export of Tetra-mt-HA but did increase export of Lyn-HA (Fig. 3B-D). These results suggest that the lack of the charged residues in the C-lobe leads to Golgi accumulation of Lyn through an insufficient association of Lyn with ACSL3.

Role of the ACSL3-LR1 domain in Golgi export of Lyn

ACSL3, a membrane-bound protein with a C-terminal large cytoplasmic portion, has a short N-terminal portion, a transmembrane domain (TM), a luciferase-like region (LR) 1 domain, which contains the phosphate-binding P-loop and the fatty acid Gate-domain, and an LR2 domain, which contains the adenine-binding motif and the long chain acyl-CoA synthetase signature motif (Fujino et al., 1997; Black et al., 1997; Soupene and Kuypers,

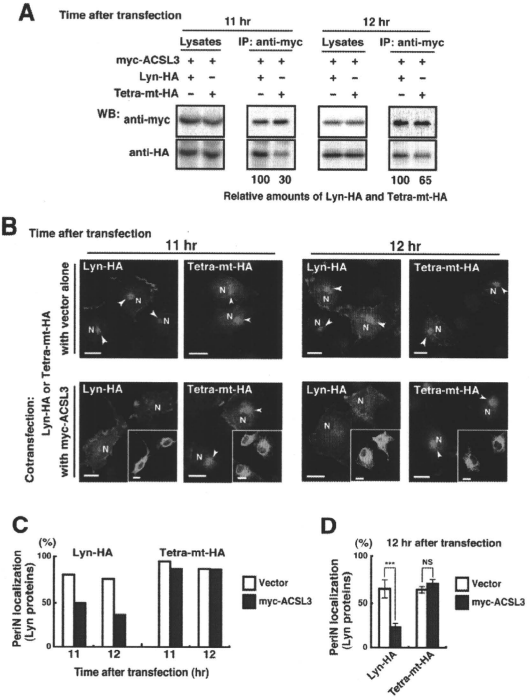

Fig. 3. Role of the C-lobe charged residues in Lyn trafficking. COS-1 cells transfected with Lyn-HA alone, Lyn-HA plus Myc-ACSL3, Tetra-mt-HA alone or Tetra-mt-HA plus Myc-ACSL3 were cultured for 11 or 12 hours. (**A**) Myc-ACSL3 was immunoprecipitated from Triton X-100 cell lysates with anti-Myc antibody, and immunoblotting was performed for Myc and HA. Amounts of Tetra-mt-HA that were coimmunoprecipitated with Myc-ACSL3 are expressed as values relative to those of Lyn-HA after normalization with Myc-ACSL3 protein levels. (**B**) Cells were doubly stained with anti-HA (red) and anti-Myc (green) antibodies. Insets show fluorescence images of Myc-ACSL3. Arrowheads indicate the perinuclear region. N, nucleus. Scale bars: 20 μm. (**C**) Cells exhibiting predominant perinuclear localization of Lyn-HA and Tetra-mt-HA were quantified 11 hours and 12 hours after transfection, and results were obtained from a representative experiment (n>200). (**D**) Cells exhibiting predominant perinuclear localization of Lyn-HA and Tetra-mt-HA were quantified 12 hours after transfection, and results (%) represent means ± s.d. from three independent experiments (n>200). Asterisks indicate the significant difference (***P<0.001; NS, not significant) calculated by Student's t-test.

2008). To examine a region in ACSL3 responsible for Lyn trafficking, we constructed two Myc-ACSL3 mutants lacking the LR2 (Myc-ΔLR2) or LR1 domain (Myc-ΔLR1) (Fig. 4A). When COS-1 cells were cotransfected with Lyn-HA and each Myc-ACSL3 mutant, we showed that Lyn-HA was indeed coimmunoprecipitated with Myc-ΔLR2 but not Myc-ΔLR1 (Fig. 4B). Next, we cotransfected COS-1 cells with Lyn-HA and each Myc-ACSL3 mutant and examined their localizations 12 hours after transfection. Intriguingly, Myc-ΔLR1 did not accelerate Golgi export of Lyn-HA, whereas Myc-ΔLR2 significantly accelerated Golgi export of Lyn-HA (Fig. 4C). However, it is of interest to note that the localizations of Myc-ΔLR2 and Myc-ΔLR1 were similar to that of Myc-ACSL3 (Fig. 4C). Given that the LR1 and LR2 domains are both required for the acyl-CoA synthetase activity (Iijima et al., 1996), these results suggest that the ACSL3 LR1 domain has a crucial role in Golgi export of Lyn through its ACSL3 association in a manner that is independent of the acyl-CoA synthetase activity.

Requirement of ACSL3 for Golgi export of Lyn

To examine whether ACSL3 was required for Golgi export of Lyn, we knocked down endogenous ACSL3 expression using short hairpin RNAs (shRNAs). To visualize shRNA-transfected cells, the mCherry expression cassette was introduced into the shRNA expression vector. Western blotting analysis showed that the protein levels of endogenous ACSL3 in HeLa cells were reduced by 56-94% at 20 hours after transfection with ACSL3-A1, ACSL3-A2 or ACSL3-A3 shRNA (Fig. 5A). When Lyn-HA was seen predominantly at the plasma membrane at 20 hours after transfection, we showed that coexpression of Lyn-HA with ACSL3-A1, ACSL3-A2 or ACSL3-A3 shRNA significantly increased the levels of Golgi localization of Lyn-HA (Fig. 5B,C). However, knockdown of ACSL3 did not affect Golgi localization of GalT and GM130 (supplementary material Fig. S5A,B). Then, to examine the effect of ACSL3 knockdown on the trafficking of endogenous Lyn, we used human megakaryocytic Dami cells in which endogenous Lyn was detectable by immunostaining (Sato et al., 2009) and found that transfection of Dami cells with ACSL3-A2 or ACSL3-A3 shRNA resulted in a ~45% reduction of endogenous ACSL3 levels (Fig. 5D). In control Dami cells, endogenous Lyn was mainly found at the plasma membrane, and a very small fraction of Lyn was seen at the Golgi (Fig. 5E, upper panels), which is consistent with our recent results (Sato et al., 2009). Intriguingly, transfection with ACSL3-A2 or ACSL3-A3 shRNA increased the levels of Golgi accumulation of

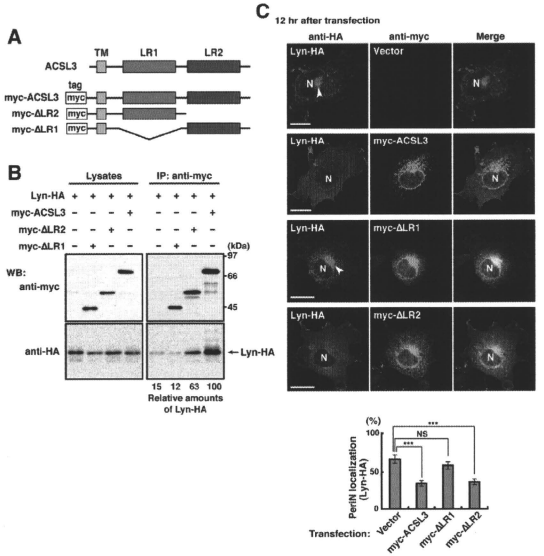

Fig. 4. Role of the LR1 domain of ACSL3 in Lyn trafficking. (**A**) Schematic representations of ACSL3 constructs with the Myc tag, the transmembrane domain (TM), and the luciferase-like regions (LR). (**B**) COS-1 cells transfected with Lyn-HA plus each Myc-ACSL3 construct were cultured for 24 hours. Each Myc-ACSL3 mutant protein was immunoprecipitated from Triton X-100 cell lysates with anti-Myc antibody, and immunoblotting was performed for Myc and HA. Molecular size markers in kDa are indicated on the right. Amounts of Lyn-HA in the Myc-ACSL3 mutant immunoprecipitates are expressed as values relative to that of Lyn-HA in the immunoprecipitate of full-length Myc-ACSL3 after normalization with protein levels of Myc-ACSL3 and its mutants. (**C**) COS-1 cells transfected with Lyn-HA in conjunction with vector alone or each ACSL3 construct were cultured for 12 hours and doubly stained with anti-HA (red) and anti-Myc (green) antibodies. Arrowheads indicate the perinuclear region. N, nucleus. Scale bars: 20 μm. Cells exhibiting predominant perinuclear localization of Lyn-HA were quantified, and results (%) represent means ± s.d. from three independent experiments (n>200). Asterisks indicate significant differences (***P<0.001; NS, not significant) calculated by Student's t-test.

endogenous Lyn, whereas transfection with control shRNA did not affect the localization of endogenous Lyn (Fig. 5E). In addition, transfection with ACSL3-A3 shRNA did not inhibit the cell-surface localization of the transmembrane protein CD43 (supplementary material Fig. S5C). These results suggest that ACSL3 is crucial for export of Lyn from the Golgi toward the plasma membrane.

Comparison of the localization of Src, Lyn and Yes upon knockdown of ACSL3

Similarly to Lyn, Yes, which is another member of the Src-family kinases, is also transported to the plasma membrane through the Golgi (Sato et al., 2009). However, Src is rapidly exchanged between the plasma membrane and late endosomes (Kasahara et al., 2007a; Kasahara et al., 2008). We thus examined the localization of Src, Lyn and Yes upon knockdown of ACSL3 in HeLa cells. We found that knockdown of ACSL3 blocked Golgi export of Yes as well as Lyn, but the knockdown did not affect the localization of Src (Fig. 6A), supported by ACSL3 association with Lyn and Yes but not Src (Fig. 6B). Note that ACSL3 knockdown inhibited plasma-membrane localization of Lyn and Yes but not Src. These results suggest that ACSL3 association is required for the trafficking of the Src-family members, such as Lyn and Yes, which are biosynthetically transported to the plasma membrane through the Golgi.

Golgi export of Lyn and VSV-G by different post-Golgi carriers

To examine whether ACSL3 affected the conventional export route from the Golgi to the plasma membrane, we tested the effect of ACSL3 knockdown on Golgi export of vesicular stomatitis virus glycoprotein (VSV-G) in COS-1 cells. The levels of endogenous ACSL3 in COS-1 cells were reduced by 45-47% upon transfection with ACSL3-A3 shRNA, resulting in Golgi accumulation of Lyn-HA (supplementary material Fig. S6). Cells cotransfected with green fluorescent protein (GFP)-tagged VSV-G (VSV-G-GFP) plus mCherry (control) or ACSL3-A3 shRNA-mCherry were incubated at 40°C to accumulate VSV-G-GFP in the ER and then shifted to 32°C for 30 minutes or 6 hours to transport VSV-G-GFP through the Golgi to the plasma membrane. Knockdown of ACSL3 did not affect Golgi export of VSV-G-GFP (Fig. 7A), suggesting that Golgi export of VSV-G-GFP is independent of ACSL3.

To further examine whether Lyn and VSV-G could be sorted into different post-Golgi transport carriers (PGCs), COS-1 cells cotransfected with Lyn-wt and VSV-G-GFP were treated with tannic acid, which inhibits fusion of PGCs with the plasma membrane to accumulate PGCs (Polishchuk et al., 2004). Tannic acid treatment enabled us to visualize PGCs containing Lyn-wt at the cell periphery (Fig. 7B). Intriguingly, most PGCs containing Lyn-wt were different to those carrying VSV-G-GFP and were also different to caveolin-positive PGCs. Consistent with our observations that Lyn is colocalized with caveolin at the Golgi but not at the cell periphery (Kasahara et al., 2004; Ikeda et al., 2009), these results suggest that Lyn is exported from the Golgi by unconventional PGCs.

Next, to examine how ACSL3 is involved in Golgi export of Lyn, COS-1 cells cotransfected with Lyn-wt, VSV-G-GFP and Myc-ACSL3 were treated with tannic acid. We found that ACSL3 overexpression significantly increased the number of PGCs containing Lyn-wt but not that of PGCs carrying VSV-G-GFP (Fig. 7C). However, tannic acid treatment did not affect the localization of Myc-ACSL3, and at the cell periphery Myc-ACSL3 did not colocalize with PGCs containing Lyn-wt. These results

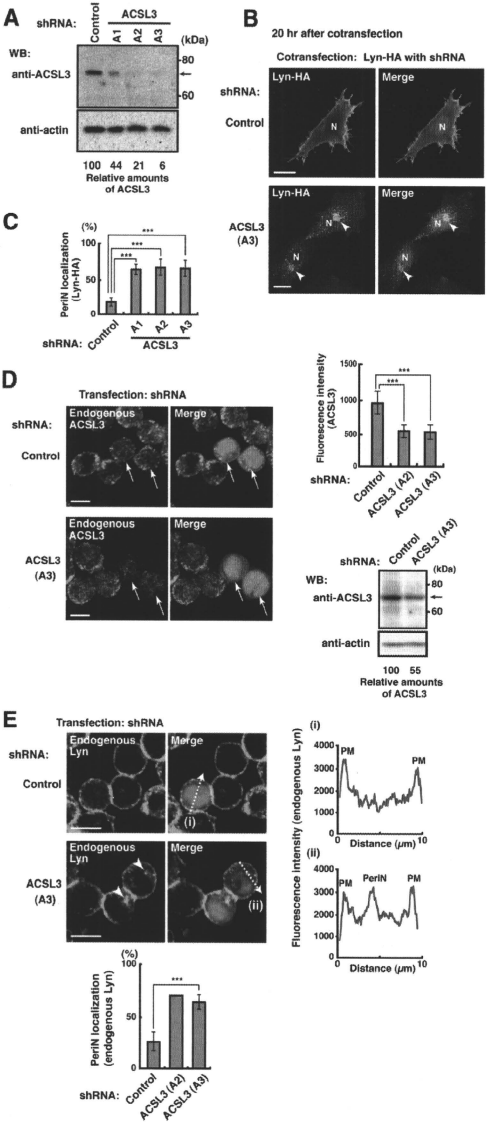

Fig. 5. Blockade of Golgi export of Lyn by ACSL3 knockdown. (**A**) HeLa cells were transfected with control shRNA-mCherry vector or ACSL3 shRNA (ACSL3-A1, ACSL3-A2 or ACSL3-A3)-mCherry vector and cultured for 20 hours. Triton X-100 cell lysates were immunoblotted for ACSL3 and actin. Amount of ACSL3 is expressed relative to that in the control cell lysate after normalization with actin levels. Molecular size markers in kDa are indicated on the right. (**B**,**C**) HeLa cells were cotransfected with Lyn-HA in conjunction with control shRNA-mCherry vector or ACSL3 shRNA (ACSL3-A1, ACSL3-A2 or ACSL3-A3)-mCherry vector and cultured for 20 hours. Expressed proteins were visualized with anti-HA antibody (green) and mCherry fluorescence (red). Arrowheads indicate the perinuclear region. N, nucleus. Scale bars: 20 μm. Cells exhibiting predominant perinuclear localization of Lyn-HA were quantified, and results (%) represent means ± s.d. from three independent experiments. Asterisks indicate the significant difference (***P<0.001) calculated by Student's t-test. (**D**) Dami cells were transfected with control shRNA-mCherry vector or ACSL3 shRNA (ACSL3-A2 or ACSL3-A3)-mCherry vector and cultured for 20 hours. Cells were stained with anti-ACSL3 antibody (green). Arrows indicate cells transfected with shRNA-mCherry vector. Scale bars: 10 μm. Mean fluorescence intensity of anti-ACSL3 staining in individual cells was measured, and results represent means ± s.d. from ~18-49 cells (n=48 for control; n=18 for ACSL3-A2; n=49 for ACSL3-A3; ***P<0.001). Triton X-100 cell lysates were immunoblotted for ACSL3 and actin, and amounts of ACSL3 are expressed as values relative to that in control. Molecular size markers in kDa are indicated on the right. (**E**) Dami cells transfected with control shRNA-mCherry vector or ACSL3 shRNA (ACSL3-A2 or ACSL3-A3)-mCherry vector were cultured for 20 hours. Endogenous Lyn and mCherry were visualized with anti-Lyn antibody (green) and mCherry fluorescence (red). Intensity plots along the dotted lines (i, ii) are shown for endogenous Lyn (green line). Arrowheads indicate the perinuclear region. Scale bars: 10 μm. PM, plasma membrane; PeriN, perinuclear region. Cells exhibiting perinuclear localization of endogenous Lyn were quantified, and results (%) represent means ± s.d. from three independent experiments (n>200). The result of ACSL3-A2 shRNA was obtained from a representative experiment (n=200). Asterisks indicate the significant difference (***P<0.001) calculated by Student's t-test.

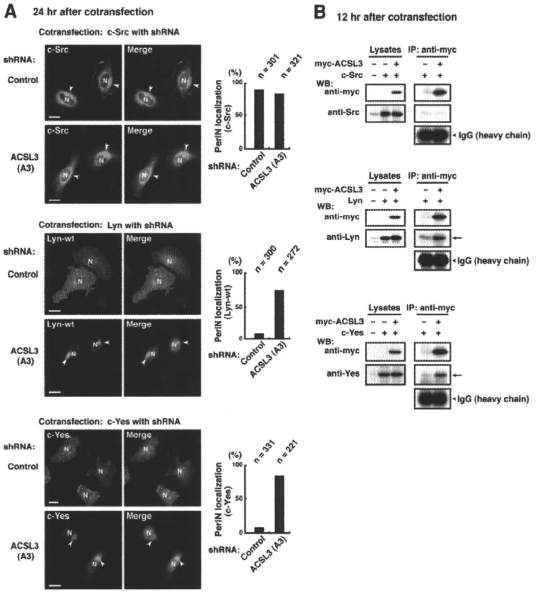

Fig. 6. Trafficking of Lyn and Yes, but not Src is regulated by ACSL3 association. (**A**) HeLa cells cotransfected with control or ACSL3-A3 shRNA in conjunction with Src, Lyn-wt, and Yes were cultured for 24 hours. Expressed proteins were visualized with anti-Src, anti-Lyn or anti-Yes antibody (green) and mCherry (red) fluorescence. Cells exhibiting perinuclear localization of Src, Lyn and Yes were quantified from three representative experiments (n>200). Arrowheads indicate the region containing late endosomes and lysosomes (Src) or Golgi region (Lyn and Yes) as described recently (Kasahara et al., 2007a; Kasahara et al., 2007b; Kasahara et al., 2008; Sato et al., 2009). N, nucleus. Scale bars: 20 μm. (**B**) COS-1 cells cotransfected with Src, Lyn-wt or Yes in conjunction with vector alone or Myc-ACSL3 were cultured for 12 hours. Myc-ACSL3 were immunoprecipitated from Triton X-100 cell lysates with anti-Myc antibody. Immunoblotting was performed for Myc, Src, Lyn and Yes. Arrows indicate coimmunoprecipitated bands.

suggest that ACSL3 has a key role in triggering Golgi export of Lyn on Golgi membranes through an increase in the number of a specific subset of PGCs that contain Lyn.

Discussion

In the present study, we provide evidence that a novel protein-protein interaction mediated by the Lyn kinase domain has a crucial role in the trafficking of newly synthesized Lyn. First, the Lyn kinase C-lobe is associated with ACSL3 and the association is inhibited by the lack of the four charged amino acid residues in the Lyn kinase C-lobe. Second, the association of Lyn with ACSL3 is inhibited by CSK-induced closed conformation, where the four charged amino acid residues are masked. Third, overexpression of CSK induces Golgi accumulation of Lyn, whereas overexpression of ACSL3 accelerates Golgi export of Lyn toward the plasma membrane. Fourth, the LR1 domain of ACSL3 is sufficient for association with Lyn and acceleration of Golgi export of Lyn. Fifth, Golgi export of Lyn but not VSV-G is blocked by ACSL3 knockdown and mediated by PGCs distinct from those carrying VSV-G. We show for the first time the significance of the Lyn kinase domain in an open conformation for Golgi export of newly synthesized Lyn through association with ACSL3.

Thus, we present a model for Golgi export of Lyn initiated by the association of the ACSL3 LR1 domain with the Lyn C-lobe in when Lyn is in an open conformation (Fig. 8). Newly synthesized Lyn in the cytoplasm is accumulated on Golgi membranes. In a closed conformation, mediated by CSK-catalyzed phosphorylation of the C-terminal tyrosine residue, Lyn is unable to associate with ACSL3 and remains on Golgi membranes. Once Lyn forms an open conformation by dephosphorylation of the tyrosine-phosphorylated tail, Lyn is associated with ACSL3 via the kinase C-lobe and is then released from Golgi membranes toward the plasma membrane while undergoing dissociation from ACSL3.

Src-family tyrosine kinases have modular domains for protein-protein interactions, such as the SH3 and SH2 domains (Pawson, 1995). The SH3 and SH2 domains of Src-family kinases have an important role in their localization, such as focal adhesions, lysosomes, late endosomes and the Golgi (Kaplan et al., 1994; Kasahara et al., 2007a; Kasahara et al., 2008; Li et al., 2008; Ikeda et al., 2009). The kinase domain of Src-family tyrosine kinases is believed to solely exert the catalytic activity. Nonetheless, we have shown that the Lyn kinase C-lobe, but not kinase activity, is required for the proper trafficking of Lyn from the Golgi (Kasahara et al., 2004) and the targeting of Lyn to the Golgi pool of caveolin (Ikeda et al., 2009). In fact, our results shown in Figs 1-3 substantiate a protein-protein interaction through the C-lobe of the Lyn kinase domain by identifying a binding partner of the C-lobe. This unusual kinase-domain-mediated protein-protein interaction is emphasized by the findings that the association of Lyn with ACSL3 is inhibited by CSK-mediated phosphorylation of the C-terminal tyrosine residue of Lyn (Fig. 1F; Fig. 2D,G) and the kinase activity of Lyn is dispensable for the association (Fig. 1E). Given that four negative-charged amino acid residues on the αE and αI helices in the C-lobe intramolecularly interact with three positively charged amino acid residues on the αA helix in the SH2 domain in a closed conformation (Sicheri et al., 1997; Xu et al.,

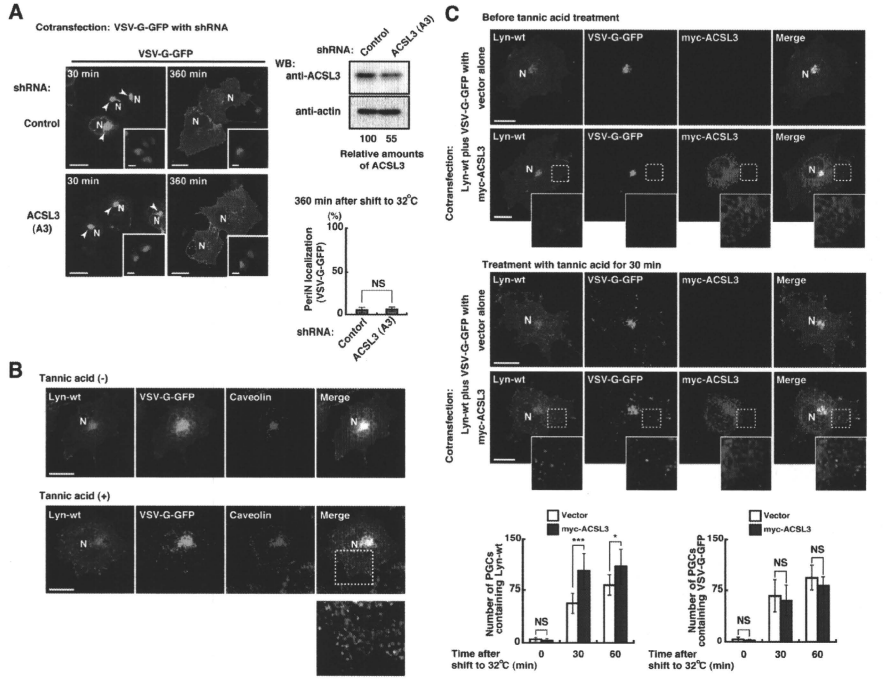

Fig. 7. Golgi exit of Lyn and VSV-G through different post-Golgi carriers. (**A**) COS-1 cells cotransfected with VSV-G-GFP in conjunction with mCherry vector (control) or ACSL3-A3 shRNA-mCherry vector were incubated at 40°C for 14 hours and then shifted to 32°C for 360 minutes, with cycloheximide for the last 3 hours. Triton X-100 cell lysates prepared before cycloheximide treatment were immunoblotted for ACSL3 and actin. Amount of ACSL3 is expressed relative to that in the control cell lysate after normalization with actin levels. Expressed proteins at 30 or 360 minutes after shift to 32°C were visualized with GFP (green) and mCherry (red) fluorescence. Insets show fluorescence images of mCherry. Arrowheads indicate the perinuclear region. N, nucleus. Scale bars: 20 μm. Cells exhibiting predominant perinuclear localization of VSV-G-GFP at 360 minutes after shift to 32°C were quantified, and results (%) represent means ± s.d. from three independent experiments. The difference between mCherry (control) and ACSL3-A3 shRNA-mCherry was not significant (NS), as calculated by Student's *t*-test. (**B**) COS-1 cells cotransfected with Lyn-wt plus VSV-G-GFP were incubated for 9 hours at 40°C and then shifted to 19°C for 2 hours to accumulate both proteins in the Golgi. Subsequently, cells were cultured at 32°C for 1 hour in the presence or absence of tannic acid. Lyn-wt (red), caveolin (blue) and VSV-G-GFP (green) were visualized with appropriate antibody and GFP fluorescence. Magnified image of a squared area is shown. N, nucleus. Scale bars: 20 μm. (**C**) COS-1 cells were cotransfected with Lyn-wt plus VSV-G-GFP in conjunction with vector alone or Myc-ACSL3. Cells incubated for 7 hours at 40°C were shifted to 19°C for 2 hours and subsequently treated with tannic acid for the indicated times. Expressed proteins were visualized with anti-Lyn (red) and anti-Myc (blue) antibodies and GFP fluorescence (green). N, nucleus. Scale bars: 20 μm. Insets show magnified images of squared areas. The number of post-Golgi carriers was counted at the indicated times. Results represent means ± s.d. from 15 or 25 cells (n=15 for 0 and 60 minutes; n=25 for 30 minutes). Asterisks indicate significant differences (*P<0.05; ***P<0.001; NS, not significant) calculated by Student's *t*-test.

1997; Kasahara et al., 2004), an open conformation of Lyn unmasks the αE and αI helices in the C-lobe for an association with ACSL3.

The mammalian ACSL family has five members with different localizations: ACSL1, in the ER and the cytosol; ACSL3, in the ER and the Golgi (this study); ACSL4 and ACSL5, in mitochondria; and ACSL6, in the plasma membrane (Lewin et al., 2001; Soupene and Kuypers, 2008). Long chain acyl-CoA, which is generated by the catalytic activity of ACSL, is required for budding of transport vesicles from Golgi membranes (Glick and Rothman, 1987; Pfanner et al., 1989; Barr and Shorter, 2000). The ACSL3 activity is also required for very low-density-lipoprotein-mediated secretion of hepatitis C virus particles in hepatoma cells (Yao and Ye, 2008). However, given that the ACSL-LR1 domain per se does not exert the catalytic activity (Iijima et al., 1996; Black et al., 1997; Soupene and Kuypers, 2008), ACSL3 is likely to act as a component of a hypothetical initiator complex for Golgi export of Lyn and might function as an adaptor protein on Golgi membranes.

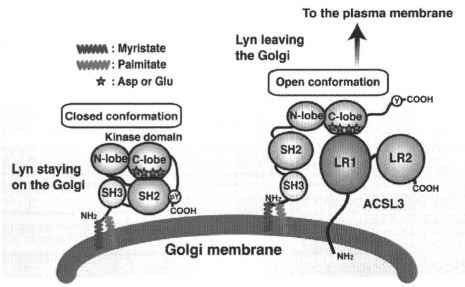

Fig. 8. A model for Golgi export of Lyn through an interaction of the C-lobe with ACSL3. In the 'closed conformation' induced by CSK, Lyn is unable to associate with ACSL3, thereby remaining on Golgi membranes. In the 'open conformation' of Lyn created by dephosphorylation of the C-terminal tail, exposure of the four negative-charged residues in the C-lobe of the kinase domain to the molecular surface facilitates the association of the C-lobe with the ACSL3-LR1 domain, leading to initiation of Lyn export from the Golgi toward the plasma membrane.

Lck, another member of the Src family, travels from the perinuclear region to the plasma membrane all the way with specific transport carriers containing MAL in T cells (Antón et al., 2008). In contrast to MAL, ACSL3 has a unique character to physically associate with Lyn on the Golgi and remain on the Golgi without formation of ACSL3-positive PGCs (Figs 1,2,7; supplementary material Fig. S2). These results suggest that unlike MAL in Lck trafficking, ACSL3 association with newly synthesized Lyn takes place on the Golgi, and ACSL3 is released from Lyn when Lyn leaves the Golgi. Presumably, ACSL3 can trigger and stimulate Golgi export of Lyn but not deliver Lyn from the Golgi to the plasma membrane.

It is of interest to note that formation of PGCs containing Lyn but not those carrying VSV-G is stimulated by ACSL3 (Fig. 7C), and that Lyn and caveolin are sorted into different PGCs despite their colocalization at the Golgi (Fig. 7B). Given that VSV-G and caveolin are sorted into separate PGCs and destined for different plasma membrane domains (Presley et al., 1997; Tagawa et al., 2005; Hayer et al., 2010), the targeting of Lyn toward a specific domain(s) of the plasma membrane could be directed by ACSL3-dependent transport.

Recently, we showed that Lyn and Yes, which are monopalmitoylated Src-family kinases, are transported to the plasma membrane through the Golgi (Sato et al., 2009), whereas Src, which is nonpalmitoylated Src-family kinase, is rapidly exchanged between the plasma membrane and late endosomes or lysosomes (Kasahara et al., 2007a). Intriguingly, Yes but not Src, is indeed associated with ACSL3, and Golgi export of Yes is blocked by ACSL3 knockdown, but the localization of Src is not affected (Fig. 6), leading to the hypothesis that ACSL3 association is required for the trafficking of the monopalmitoylated Src-family member that are biosynthetically transported to the plasma membrane via the Golgi. Given that Lyn and Yes have a crucial role in signal transduction mostly at the cytoplasmic face of the plasma membrane upon extracellular ligand stimulation (Thomas and Brugge, 1997), ACSL3 is indispensable for plasma membrane localization of Lyn and Yes. Lyn is known to participate in the B-cell-antigen receptor (BCR) and FcεRI signaling at the plasma membrane in B-cells and mast cells, respectively (Nishizumi et al., 1995; Bolen and Brugge, 1997; Thomas and Brugge, 1997; Sheets et al., 1999; Rivera and Olivera, 2007; Sohn et al., 2008). Presumably, the association of Lyn with ACSL3 has a crucial role in proper Lyn localization to the plasma membrane, which leads to the appropriate BCR and FcεRI signaling. Moreover, it is shown that Golgi membranes can serve as a platform of Src-family kinases for signal transduction: Golgi-localized Lyn tyrosine-phosphorylates annexin II on Golgi membranes under oxidative stress (Matsuda et al., 2006) and Golgi-localized Lck is needed for the activation of Raf-1 under weak stimulation through the T-cell receptor (Li et al., 2008). Thus, ACSL3 might be involved in regulation of the balance of localization of Lyn and Yes between the plasma membrane and Golgi membranes.

In conclusion, we show that Golgi export of Lyn requires the association of the Lyn kinase C-lobe with ACSL3 when Lyn is in its open conformation. Despite the high homology of Src-family kinases, the localization of Lyn and Yes but not Src is affected by the lack of ACSL3, suggesting the importance of spatio-temporal localization of the Src-family kinases. It would be interesting to look for a possible protein complex, including Lyn and ACSL3, on Golgi membranes to determine which factors are responsible for regulating initiation of Golgi export of Lyn and to determine whether ACSL3 is involved in the trafficking of other proteins from the Golgi to the plasma membrane.

Materials and Methods

Plasmids

cDNAs encoding human wild-type Lyn (Lyn-wt) (1-512; with 1 designating the initiator methionine) and human wild-type Yes (1-543) were provided by Tadashi Yamamoto (The University of Tokyo, Tokyo, Japan) (Yamanashi et al., 1987; Sukegawa et al., 1987). cDNA encoding human wild-type Src (1-536) (Biorge et al., 1995) (provided by Donald J. Fujita, University of Calgary, Calgary, Canada) was previously described (Kasahara et al., 2007b). Three HA-tagged Lyn constructs lacking the C-terminal negative-regulatory tail, Lyn-HA (1-506; kinase-active), Lyn(K275A)-HA(1-506; kinase-dead) and Tetra-mt-HA (1-506; Asp346→Ala, Glu353→Ala, Asp498→Ala, Asp499→Ala), were described previously (Kasahara et al., 2004). For protein expression, all constructs were subcloned into the pcDNA4/TO vector (Invitrogen). Human ACSL3 cDNA subcloned into the pBluescript vector (Stratagene) was provided by Takahiro Fujino (Ehime University, Matsuyama, Japan) (Minekura et al., 1997). To construct N-terminally Myc-tagged ACSL3 (Myc-ACSL3), the *Sac*I-*Not*I fragment containing full-length ACSL3 was ligated into the *Sac*II (blunted) and *Not*I sites of pcDNA3-Myc-cyclinA-GFP (Clute and Pines, 1999; provided by Jonathon Pines, Gurdon Institute, Cambridge, UK). The resulting Myc-ACSL3 cDNA was subcloned into pcDNA4/TO, and removal of the Zeocin-resistant gene generated pcDNA4/TO-Myc-ACSL3(ΔZeo'). The spacer sequence MVGNSAPGPATREAGSALLALQQTALQEDQENINPEKAAPVQQPL was inserted between the Myc tag and ACSL3. Myc-ACSL3ΔLR2 (1-444) was generated from pcDNA4/TO-Myc-ACSL3(ΔZeo') by *Ssp*I and *Not*I digestion and blunting. To construct Myc-ACSL3ΔLR1 (1-94 and 438-720), the *Nde*I (blunted) and *Bsst*BI (blunted) fragment of pcDNA4/TO-Myc-ACSL3(ΔZeo') was replaced with the *Sal*I (blunted)-*Xho*I (blunted) fragment of pBluescript as a spacer encompassing three amino acid residues (RPR). Rat *Csk* cDNA subcloned into the pME18S vector was provided by Masato Okada and Shigeyuki Nada (Osaka University, Osaka, Japan)

Journal of Cell Science

(Nada et al., 1991). The plasmid for vesicular stomatitis virus glycoprotein fused to green fluorescent protein (VSV-G-GFP) was provided by Jennifer Lippincott-Schwartz (National Institutes of Health, Bethesda, MD) (Presley et al., 1997) through Mitsuo Tagaya (Tokyo University of Pharmacy and Life Sciences, Tokyo, Japan) (Hirose et al., 2004). A glutathione-S-transferase-fusion protein containing the Lyn C-lobe (326-506) (GST-C-lobe) was constructed by subcloning the Lyn C-lobe between the *Bam*HI (blunted) and *Sma*I sites of the pGEX-5X2 vector (Amersham Biosciences). GST-C-lobe-mt (326-506; Asp346→Ala, Glu353→Ala, Asp498→Ala, Asp499→Ala) was constructed by replacing the C-lobe with the C-lobe-mt of Tetra-mt-HA.

Antibodies

The following antibodies were used: HA epitope (F-7 and Y-11; Santa Cruz Biotechnology), Myc epitope (PL14; Medical & Biological Laboratory, Nagoya, and 9E10 and A-14; Santa Cruz Biotechnology), Lyn (Lyn44 and H-6; Santa Cruz Biotechnology, and Lyn9; Wako Pure Chemicals, Osaka, Japan), CSK (#52; BD Transduction Laboratories), actin (MAB1501; Chemicon International), Src (#327; Oncogene Research, GD11; Millipore), Src phosphorylated on Y416 (Src-P-family; Cell Signaling Technology), Yes (#1; BD Biosciences), GM130 (#35, BD Biosciences), GalT (Yamaguchi and Fukuda, 1995) (provided by Michiko N. Fukuda, The Burnham Institute for Medical Research, La Jolla, CA), caveolin (Transduction Laboratories), calnexin (Stressgen Bioreagents), and CD43 (MEM59, Sanbio B.V.). MOPC21 (Sigma) was used for mouse control IgG. Rabbit anti-ACSL3 antiserum was generated against a GST-fusion protein containing the N-terminal amino acid residues (70-259) of human ACSL3 (Fujimoto et al., 2004) (provided by Y. Fujimoto and T. Takano, Teikyo University, Tokyo, Japan) and extensively absorbed with GST before use. Horseradish peroxidase (HRP)-F(ab′)$_2$ of anti-mouse IgG, anti-rabbit Ig and anti-rat IgG secondary antibodies were from Amersham Biosciences. FITC-F(ab′)$_2$ of anti-rabbit IgG or of anti-mouse IgG, TRITC-anti-rabbit IgG, TRITC-anti-mouse IgG (Fc specific) and Alexa Fluor 647-anti-rabbit IgG secondary antibodies were from BioSource International, Sigma and Invitrogen.

Cells and transfection

HeLa (Japanese Collection of Research Bioresource, Osaka, Japan) and COS-1 cells were cultured in Iscove's modified DME containing 5% fetal bovine serum at 37°C. THP-1 cells (provided by Atsushi Iwama, Chiba University, Chiba, Japan) were grown in suspension in Iscove's modified DME containing 5% fetal bovine serum and 50 μM 2-mercaptoethanol, and Dami cells were maintained in suspension culture in Iscove's modified DME supplemented with 7.5% horse serum, as described (Greenberg et al., 1988; Hirao et al., 1998; Sato et al., 2009), and attached to culture dishes during ~2-3 days of culture in Iscove's modified DME supplemented with 2.5% fetal bovine serum and 2.5% horse serum. Transient transfection was performed using *Trans*IT transfection reagent (Mirus), LipofectAMINE™ 2000 reagent (Invitrogen) or linear polyethylenimine (25 kDa; Polysciences) (Matsuda et al., 2006; Kasahara et al., 2007a; Fukumoto et al., 2010).

Western blotting and immunoprecipitation

Cell lysates were prepared in SDS-PAGE sample buffer or Triton X-100 lysis buffer (50 mM HEPES, pH 7.4, 10% glycerol, 1% Triton X-100, 4 mM EDTA, 100 mM NaF, 50 μg/ml aprotinin, 100 μM leupeptin, 25 μM pepstatin A, and 2 mM PMSF), and subjected to SDS-PAGE and electrotransferred onto polyvinylidene difluoride membranes (Millipore). Immunodetection was performed by enhanced chemiluminescence (Amersham Biosciences), as described (Yamaguchi et al., 2001; Kasahara et al., 2004; Matsuda et al., 2006; Kasahara et al., 2007b; Ikeda et al., 2008; Kuga et al., 2008; Sato et al., 2009). Sequential reprobing of membranes with a variety of antibodies was performed after the complete removal of primary and secondary antibodies from membranes in stripping buffer or inactivation of HRP by 0.1% NaN_3, according to the manufacturer's instructions. Results were analyzed using an image analyzer LAS-1000plus equipped with Science Lab software (Fujifilm, Tokyo, Japan) or ChemiDoc XRSPlus (Bio-Rad). Immunoprecipitation was performed using antibody-precoated protein-G beads, as described (Mera et al., 1999; Yamaguchi et al., 2001; Kasahara et al., 2004; Kasahara et al., 2007b; Ikeda et al., 2008; Sato et al., 2009). Intensity of chemiluminescence was measured using the ImageJ software (NIH, USA).

GST-pulldown assay

GST-fusion proteins were expressed in the *E. coli* AD202 strain (Nakano et al., 1993) (provided by Takashi Saito, RIKEN, Yokohama, Japan) upon incubation with 0.1 mM IPTG at 30°C for 3 hours. After bacteria were lysed at 4°C in phosphate-buffered saline (PBS) containing 1% Triton X-100, the Triton X-100-insoluble fraction was lysed at 4°C with Empigen lysis buffer (50 mM HEPES, pH 7.4, 10% glycerol, 3% Empigen BB, 4 mM EDTA, 100 mM NaF, 50 μg/ml aprotinin, 100 μM leupeptin, 25 μM pepstatin A, and 2 mM PMSF), as described previously (Yamaguchi et al., 2001). GST-fusion proteins were collected on glutathione-Sepharose beads from Empigen lysates and washed four times with Empigen lysis buffer. To identify proteins associated with the C-lobe, a pulldown assay was performed at 4°C for 2 hours in Triton X-100 lysates prepared from HeLa cells. After extensively washing with Triton X-100 lysis buffer, the bead pellets were analyzed by SDS-PAGE and Coomassie brilliant blue (CBB) staining.

Identification of p70 by peptide mapping

Proteins pulled down with GST-C-lobe were resolved by SDS-PAGE using 7% acrylamide and 2.7% bisacrylamide to increase separation of p70 and stained with CBB. The protein band corresponding to p70 was cut out and digested with *Achromobacter* protease I (Lys-C) in digestion buffer (100 mM Tris-HCl, pH 9.0, 1 mM EDTA, and 0.1% SDS). After the digestion, molecular mass analysis of Lys-C fragments was performed by matrix-assisted laser desorption-ionization time-of-flight mass spectrometry (MALDI-TOF-MS). Identification of protein was carried out by comparison between the molecular weights determined by MALDI-TOF-MS and theoretical masses from the proteins registered in NCBInr.

Immunofluorescence

Immunofluorescence staining was performed as described (Yamaguchi and Fukuda, 1995; Tada et al., 1999; Nakayama and Yamaguchi, 2005; Kasahara et al., 2007c; Ikeda et al., 2008; Sato et al., 2009). In brief, cells were washed in warmed PBS and fixed in 4% paraformaldehyde for 20 minutes. Fixed cells were permeabilized and blocked in PBS containing 0.1% saponin and 3% bovine serum albumin for 30 minutes, and then incubated with a primary and a secondary antibody for 1 hour each. After washing with PBS containing 0.1% saponin, cells were mounted with ProLong antifade reagent (Molecular Probes). Confocal images were obtained using a Fluoview FV500 laser-scanning microscope with a ×40 1.00 NA oil-immersion objective (Olympus, Tokyo). 200-400 cells were scored for each assay. For immunofluorescence of THP-1 cells, cells in suspension were directly fixed with 4% paraformaldehyde and then attached onto coverslips by cytocentrifugation. Composite figures were prepared using Photoshop 11.0 and Illustrator 14.0 software (Adobe). Intensity of fluorescence was measured using the ImageJ software.

Tannic acid treatment

COS-1 cells cotransfected with Lyn-wt and VSV-G-GFP were incubated overnight at 40°C and then shifted to 19°C for 2 hours to accumulate both proteins in the Golgi. Subsequently, cells were treated with 0.5% tannic acid for 30 or 60 minutes at 32°C and fixed for confocal microscopy, as described (Polishchuk et al., 2004). After background subtraction using the ImageJ software, the number of PGCs containing Lyn-wt or VSV-G-GFP was counted from 15-25 cells.

ACSL3 gene silencing with shRNAs

Three different target-specific short hairpin RNA (shRNA) sequences were selected for silencing *ACSL3* with help of web-based algorithms (http://www.clontech.com/) (ACSL3-A1, GCTGAAACGCAAAGAGCTT; ACSL3-A2, GACCAACAT-CGCCATCTTC; ACSL3-A3, CTCTTACAAACAAAGTTGA). EGFP-targeted shRNA was used as a control shRNA (GGCAAGCTGACCCTGAAGTTCA). The oligonucleotides for shRNA were annealed and subcloned into the *Xba*I and *Bgl*II sites of the pENTR4-H1 vector (provided by Hiroyuki Miyoshi, RIKEN BRC, Tsukuba, Japan). To visualize cells that were transfected with shRNA encoding pENTR4-H1, an mCherry-coexpressing shRNA vector was constructed. In brief, the mCherry vector was constructed from the pEGFP-C1 vector (Clontech) by replacing EGFP with the monomeric red fluorescent protein mCherry of the pRSET-B-mCherry vector (Shaner et al., 2004) (provided by Roger Y. Tsien, University of California, San Diego, CA), and the H1 promoter-driven shRNA cassette of pENTR4-H1 was subsequently inserted into the mCherry vector. The resulting shRNA-mCherry vector encodes both shRNA and mCherry. When shRNA-mCherry vectors were transiently transfected, the transfection efficiencies of shRNA were 47-71% in HeLa and COS-1 cells and 5-10% in Dami cells when we counted the number of cells expressing mCherry under a confocal laser-scanning microscope.

VSV-G-GFP transport assay

COS-1 cells cotransfected with VSV-G-GFP in conjunction with mCherry (control) or ACSL3-A3 shRNA-mCherry vector were incubated at 40°C for 14 hours and then shifted to 32°C for 30 minutes or 6 hours in the presence of 200 μg/ml cycloheximide for the last 3 hours, as described (Hirschberg et al., 1998; Hirose et al., 2004; Sato et al., 2009).

We thank Tadashi Yamamoto, Takahiro Fujino, Masato Okada, Shigeyuki Nada, Hiroyuki Miyoshi, Jennifer Lippincott-Schwartz, Mitsuo Tagaya, Roger Y. Tsien, Jonathon Pines, Takashi Saito, Atsushi Iwama, Tatsuya Takano and Yasuyuki Fujimoto for plasmids, cells and antibody. This work was supported in part by grants-in-aid for Scientific Research, Global COE Program (Global Center for Education and Research in Immune Regulation and Treatment) and Special Funds for Education and Research (Development of SPECT probes for Pharmaceutical Innovation) from the Japanese Ministry of Education, Culture, Sports, Science and Technology, and research grants from the Suzuken Memorial Foundation and the Mochida Memorial Foundation for Medical and Pharmaceutical Research. Y.O. is a Global COE Research Assistant.

Supplementary material available online at
http://jcs.biologists.org/cgi/content/full/123/15/2649/DC1

References

Antón, O., Batista, A., Millán, J., Andrés-Delgado, L., Puertollano, R., Correas, I. and Alonso, M. A. (2008). An essential role for the MAL protein in targeting Lck to the plasma membrane of human T lymphocytes. *J. Exp. Med.* **205**, 3201-3213.

Barr, F. A. and Shorter, J. (2000). Membrane traffic: Do cones mark sites of fission? *Curr. Biol.* **10**, 141-144.

Bijlmakers, M. J. E., Isobe-Nakamura, M., Ruddock, L. J. and Marsh, M. (1997). Intrinsic signals in the unique domain target $p56^{lck}$ to the plasma membrane independently of CD4. *J. Cell Biol.* **137**, 1029-1040.

Biorge, J. D., Bellagamba, C., Cheng, H. C., Tanaka, A., Wang, J. H. and Fujita, D. J. (1995). Characterization of two activated mutants of human $pp60^{c\text{-}Src}$ that escape c-Src kinase regulation by distinct mechanisms. *J. Biol. Chem.* **270**, 24222-24228.

Black, P. N., Zhang, Q., Weimar, J. D. and DiRusso, C. C. (1997). Mutational analysis of a fatty acyl-coenzyme A synthetase signature motif identifies seven amino acid residues that modulate fatty acid substrate specificity. *J. Biol. Chem.* **272**, 4896-4903.

Blume-Jensen, P. and Hunter, T. (2001). Oncogenic kinase signalling. *Nature* **411**, 355-365.

Bolen, J. B. and Brugge, J. S. (1997). Leukocyte protein tyrosine kinases: potential targets for drug discovery. *Annu. Rev. Immunol.* **15**, 371-404.

Brown, M. T. and Cooper, J. A. (1996). Regulation, substrates and functions of src. *Biochim. Biophys. Acta* **1287**, 121-149.

Chu, I., Sun, J., Arnaout, A., Kahn, H., Hanna, W., Narod, S., Sun, P., Tan, C. K., Hengst, L. and Slingerland, J. (2007). p27 phosphorylation by Src regulates inhibition of cyclin E-Cdk2. *Cell* **128**, 281-294.

Clute, P. and Pines, J. (1999). Temporal and spatial control of cyclin B1 destruction in metaphase. *Nat. Cell Biol.* **1**, 82-87.

Fujimoto, Y., Itabe, H., Sakai, J., Makita, M., Noda, J., Mori, M., Higashi, Y., Kojima, S. and Takano, T. (2004). Identification of major proteins in the lipid droplet-enriched fraction isolated from the human hepatocyte cell line HuH7. *Biochim. Biophys. Acta* **1644**, 47-59.

Fujino, T., Kang, M. J., Minekura, H., Suzuki, H. and Yamamoto, T. T. (1997). Alternative translation initiation generates acyl-CoA synthetase 3 isoforms with heterogeneous amino termini. *J. Biochem.* **122**, 212-216.

Fukumoto, Y., Obata, Y., Ishibashi, K., Tamura, N., Kikuchi, I., Aoyama, K., Hattori, Y., Tsuda, K., Nakayama, Y. and Yamaguchi, N. (2010). Cost-effective gene transfection by DNA compaction at pH 4.0 using acidified, long shelf-life polyethylenimine. *Cytotechnology* 62, 73-82.

Glick, B. S. and Rothman, J. E. (1987). Possible role for fatty acyl-coenzyme A in intracellular protein transport. *Nature* **326**, 309-312.

Greenberg, S. M., Rosenthal, D. S., Greeley, T. A., Tantravahi, R. and Handin, R. J. (1988). Characterization of a new megakaryocytic cell line: the Dami cell. *Blood* **72**, 1968-1977.

Grimmler, M., Wang, Y., Mund, T., Cilensek, Z., Keidel, E. M., Waddell, M. B., Jäkel, H., Kullmann, M., Kriwacki, R. W. and Hengst, L. (2007). Cdk-inhibitory activity and stability of p27Kip1 are directly regulated by oncogenic tyrosine kinases. *Cell* **128**, 269-280.

Hayashi, T., Umemori, H., Mishina, M. and Yamamoto, T. (1999). The AMPA receptor interacts with and signals through the protein tyrosine kinase Lyn. *Nature* **397**, 72-76.

Hayer, A., Stoeber, M., Bissig, C. and Helenius, A. (2010). Biogenesis of caveolae: stepwise assembly of large caveolin and cavin complexes. *Traffic* **11**, 361-382.

Hibbs, M. L., Tarlinton, D. M., Armes, J., Grail, D., Hodgson, G., Maglitto, R., Stacker, S. A. and Dunn, A. R. (1995). Multiple defects in the immune system of Lyn-deficient mice, culminating in autoimmune disease. *Cell* **83**, 301-311.

Hirao, A., Huang, X. L., Suda, T. and Yamaguchi, N. (1998). Overexpression of C-terminal Src kinase homologous kinase suppresses activation of Lyn tyrosine kinase required for VLA5-mediated Dami cell spreading. *J. Biol. Chem.* **273**, 10004-10010.

Hirose, H., Arasaki, K., Dohmae, N., Takio, K., Hatsuzawa, K., Nagahama, M., Tani, K., Yamamoto, A., Tohyama, M. and Tagaya, M. (2004). Implication of ZW10 in membrane trafficking between the endoplasmic reticulum and Golgi. *EMBO J.* **23**, 1267-1278.

Hirschberg, K., Miller, C. M., Ellenberg, J., Presley, J. F., Siggia, E. D., Phair, R. D. and Lippincott-Schwartz, J. (1998). Kinetic analysis of secretory protein traffic and characterization of golgi to plasma membrane transport intermediates in living cells. *J. Cell Biol.* **143**, 1485-1503.

Iijima, H., Fujino, T., Minekura, H., Suzuki, H., Kang, M. J. and Yamamoto, T. (1996). Biochemical studies of two rat acyl-CoA synthetases, ACS1 and ACS2. *Eur. J. Biochem.* **242**, 186-190.

Ikeda, K., Nakayama, Y., Togashi, Y., Obata, Y., Kuga, T., Kasahara, K., Fukumoto, Y. and Yamaguchi, N. (2008). Nuclear localization of Lyn tyrosine kinase mediated by inhibition of its kinase activity. *Exp. Cell Res.* **314**, 3392-3404.

Ikeda, K., Nakayama, Y., Ishii, M., Obata, Y., Kasahara, K., Fukumoto, Y. and Yamaguchi, N. (2009). Requirement of the SH4 and tyrosine-kinase domains but not the kinase activity of Lyn for its biosynthetic targeting to caveolin-positive Golgi membranes. *Biochim. Biophys. Acta* **1790**, 1345-1352.

Kaplan, K. B., Swedlow, J. R., Varmus, H. E. and Morgan, D. O. (1992). Association of $p60^{c\text{-}src}$ with endosomal membranes in mammalian fibroblasts. *J. Cell Biol.* **118**, 321-333.

Kaplan, K. B., Bibbins, K. B., Swedlow, J. R., Arnaud, M., Morgan, D. O. and Varmus, H. E. (1994). Association of the amino-terminal half of c-Src with focal adhesions alters their properties and is regulated by phosphorylation of tyrosine 527. *EMBO J.* **13**, 4745-4756.

Kasahara, K., Nakayama, Y., Ikeda, K., Fukushima, Y., Matsuda, D., Horimoto, S. and Yamaguchi, N. (2004). Trafficking of Lyn through the Golgi caveolin involves the charged residues on αE and αI helices in the kinase domain. *J. Cell Biol.* **165**, 641-652.

Kasahara, K., Nakayama, Y., Kihara, A., Matsuda, D., Ikeda, K., Kuga, T., Fukumoto, Y., Igarashi, Y. and Yamaguchi, N. (2007a). Rapid trafficking of c-Src, a non-palmitoylated Src-family kinase, between the plasma membrane and late endosomes/lysosomes. *Exp. Cell Res.* **313**, 2651-2666.

Kasahara, K., Nakayama, Y., Sato, I., Ikeda, K., Hoshino, M., Endo, T. and Yamaguchi, N. (2007b). Role of Src-family kinases in formation and trafficking of macropinosomes. *J. Cell. Physiol.* **211**, 220-232.

Kasahara, K., Nakayama, Y., Nakazato, Y., Ikeda, K., Kuga, T. and Yamaguchi, N. (2007c). Src signaling regulates completion of abscission in cytokinesis through ERK/MAPK activation at the midbody. *J. Biol. Chem.* **282**, 5327-5339.

Kasahara, K., Nakayama, Y. and Yamaguchi, N. (2008). v-Src and c-Src, nonpalmitoylated Src-family kinases, induce perinuclear accumulation of lysosomes through Rab7 in a kinase activity-independent manner. *Cancer Lett.* **262**, 19-27.

Kuga, T., Nakayama, Y., Hoshino, M., Higashiyama, Y., Obata, Y., Matsuda, D., Kasahara, K., Fukumoto, Y. and Yamaguchi, N. (2007). Differential mitotic activation of endogenous c-Src, c-Yes, and Lyn in HeLa cells. *Arch. Biochem. Biophys.* **466**, 116-124.

Kuga, T., Hoshino, M., Nakayama, Y., Kasahara, K., Ikeda, K., Obata, Y., Takahashi, A., Higashiyama, Y., Fukumoto, Y. and Yamaguchi, N. (2008). Role of Src-family tyrosine kinases in formation of the cortical actin cap at the dorsal cell surface. *Exp. Cell Res.* **314**, 2040-2054.

Lewin, T. M., Kim, J. H., Granger, D. A., Vance, J. E. and Coleman, R. A. (2001). Acyl-CoA snthetase isoforms 1, 4, and 5 are present in different subcellular membranes in rat liver and can be inhibited independently. *J. Biol. Chem.* **276**, 24674-24679.

Ley, S. C., Marsh, M., Bebbington, C. R., Proudfoot, K. and Jordan, P. (1994). Distinct intracellular localization of Lck and Fyn protein tyrosine kinases in human T lymphocytes. *J. Cell Biol.* **125**, 639-649.

Li, M., Ong, S. S., Rajwa, B., Thieu, V. T., Geahlen, R. L. and Harrison, M. L. (2008). The SH3 domain of Lck modulates T-cell receptor-dependent activation of extracellular signal-regulated kinase through activation of Raf-1. *Mol. Cell. Biol.* **28**, 630-641.

Matsuda, D., Nakayama, Y., Horimoto, S., Kuga, T., Ikeda, K., Kasahara, K. and Yamaguchi, N. (2006). Involvement of Golgi-associated Lyn tyrosine kinase in the translocation of annexin II to the endoplasmic reticulum under oxidative stress. *Exp. Cell Res.* **312**, 1205-1217.

Mera, A., Suga, M., Ando, M., Suda, T. and Yamaguchi, N. (1999). Induction of cell shape changes through activation of the interleukin-3 common β chain receptor by the RON receptor-type tyrosine kinase. *J. Biol. Chem.* **274**, 15766-15774.

Minekura, H., Fujino, T., Kang, M. J., Fujita, T., Endo, Y. and Yamamoto, T. T. (1997). Human acyl-coenzyme A synthetase 3 cDNA and localization of its gene (ACS3) to chromosome band 2q34-q35. *Genomics* **42**, 180-181.

Möhn, H., Le Cabec, V., Fischer, S. and Maridonneau-Parini, I. (1995). The src-family protein-tyrosine kinase $p59^{hck}$ is located on the secretory granules in human neutrophils and translocates towards the phagosome during cell activation. *Biochem. J.* **309**, 657-665.

Nada, S., Okada, M., MacAuley, A., Cooper, J. A. and Nakagawa, H. (1991). Cloning of a complementary DNA for a protein-tyrosine kinase that specifically phosphorylates a negative regulatory site of $p60^{c\text{-}src}$. *Nature* **351**, 69-71.

Nakano, H., Yamazaki, T., Ikeda, M., Masai, H., Miyatake, S. and Saito, T. (1993). Purification of glutathione S-transferase fusion proteins as a non-degraded form by using a protease-negative *E. coli* strain, AD202. *Nucleic Acids Res.* **22**, 543-544.

Nakayama, Y. and Yamaguchi, N. (2005). Multi-lobulation of the nucleus in prolonged S phase by nuclear expression of Chk tyrosine kinase. *Exp. Cell Res.* **304**, 570-581.

Nishizumi, H., Taniuchi, I., Yamanashi, Y., Kitamura, D., Ilic, D., Mori, S., Watanabe, T. and Yamamoto, T. (1995). Impaired proliferation of peripheral B cells and indication of autoimmune disease in lyn-deficient mice. *Immunity* **3**, 549-560.

Pawson, T. (1995). Protein modules and signalling networks. *Nature* **373**, 573-580.

Pfanner, N., Orci, L., Glick, B. S., Amherdt, M., Arden, S. R., Malhotra, V. and Rothman, J. E. (1989). Fatty acyl-coenzyme A is required for budding of transport vesicles from Golgi cisternae. *Cell* **59**, 95-102.

Polishchuk, R., Pentima, A. D. and Lippincott-Schwartz, J. (2004). Delivery of raft-associated, GPI-anchored proteins to the apical surface of polarized MDCK cells by a transcytotic pathway. *Nat. Cell Biol.* **6**, 297-307.

Presley, J. F., Cole, N. B., Schroer, T. A., Hirschberg, K., Zaal, K. J. M. and Lippincott-Schwartz, J. (1997). ER-to-Golgi transport visualized in living cells. *Nature* **389**, 81-85.

Resh, M. D. (1994). Myristylation and palmitylation of Src family members: the fats of the matter. *Cell* **76**, 411-413.

Rivera, J. and Olivera, A. (2007). Src family kinases and lipid mediators in control of allergic inflammation. *Immunol. Rev.* **217**, 255-268.

Sato, I., Obata, Y., Kasahara, K., Nakayama, Y., Fukumoto, Y., Yamasaki, T., Yokoyama, K. K., Saito, T. and Yamaguchi, N. (2009). Differential trafficking of Src, Lyn, Yes and Fyn is specified by the state of palmitoylation in the SH4 domain. *J. Cell Sci.* **122**, 965-975.

Shaner, N. C., Campbell, R. E., Steinbach, P. A., Giepmans, B. N., Palmer, A. E. and Tsien, R. Y. (2004). Improved monomeric red, orange and yellow fluorescent proteins derived from *Discosoma sp.* red fluorescent protein. *Nat. Biotechnol.* **22**, 1567-1572.

Sheets, E. D., Holloway, D. and Baird, B. (1999). Critical role for cholesterol in Lyn-mediated tyrosine phosphorylation of FcεRI and their association with detergent-resistant membranes. *J. Cell Biol.* **145**, 877-887.

Sicheri, F., Moarefi, I. and Kuriyan, J. (1997). Crystal structure of the Src family tyrosine kinase Hck. *Nature* **385**, 602-609.

Sohn, H. W., Tolar, P. and Pierce, S. K. (2008). Membrane heterogeneities in the formation of B cell receptor-Lyn kinase microclusters and the immune synapse. *J. Cell Biol.* **182**, 367-379.

Soupene, E. and Kuypers, F. A. (2008). Mammalian long-chain acyl-CoA synthetases. *Exp. Biol. Med.* **233**, 507-521.

Sukegawa, J., Semba, K., Yamanashi, Y., Nishizawa, M., Miyajima, N., Yamamoto, T. and Toyoshima, K. (1987). Characterization of cDNA clones for the human c-yes gene. *Mol. Cell. Biol.* **7**, 41-47.

Tada, J., Omine, M., Suda, T. and Yamaguchi, N. (1999). A common signaling pathway via Syk and Lyn tyrosine kinases generated from capping of the sialomucins CD34 and CD43 in immature hematopoietic cells. *Blood* **93**, 3723-3735.

Tagawa, A., Mezzacasa, A., Hayer, A., Longatti, A., Pelkmans, L. and Helenius, A. (2005). Assembly and trafficking of caveolar domains in the cell: caveolae as stable, cargo-triggered, vesicular transporters. *J. Cell Biol.* **170**, 769-779.

Takahashi, A., Obata, Y., Fukumoto, Y., Nakayama, Y., Kasahara, K., Kuga, T., Higashiyama, Y., Saito, T., Yokoyama, K. K. and Yamaguchi, N. (2009). Nuclear localization of Src-family tyrosine kinases is required for growth factor-induced euchromatinization. *Exp. Cell Res.* **315**, 1117-1141.

Thomas, S. M. and Brugge, J. S. (1997). Cellular functions regulated by SRC family kinases. *Annu. Rev. Cell Dev. Biol.* **13**, 513-609.

Tsukita, S., Oishi, K., Akiyama, T., Yamanashi, Y., Yamamoto, T. and Tsukita, S. (1991). Specific proto-oncogenic tyrosine kinases of src family are enriched in cell-to-cell adherens junctions where the level of tyrosine phosphorylation is elevated. *J. Cell Biol.* **113**, 867-879.

Xu, W., Harrison, S. C. and Eck, M. J. (1997). Three-dimensional structure of the tyrosine kinase c-Src. *Nature* **385**, 595-602.

Yamaguchi, N. and Fukuda, M. N. (1995). Golgi retention mechanism of β-1,4-galactosyltransferase: membrane-spanning domain-dependent homodimerization and association with α- and β-tubulins. *J. Biol. Chem.* **270**, 12170-12176.

Yamaguchi, N., Nakayama, Y., Urakami, T., Suzuki, S., Nakamura, T., Suda, T. and Oku, N. (2001). Overexpression of the Csk homologous kinase (Chk tyrosine kinase) induces multinucleation: a possible role for chromatin-associated Chk in chromosome dynamics. *J. Cell Sci.* **114**, 1631-1641.

Yamanashi, Y., Fukushige, S., Semba, K., Sukegawa, J., Miyajima, N., Matsubara, K., Yamamoto, T. and Toyoshima, K. (1987). The *yes*-related cellular gene *lyn* encodes a possible tyrosine kinase similar to $p56^{lck}$. *Mol. Cell. Biol.* **7**, 237-243.

Yao, H. and Ye, J. (2008). Long chain acyl-CoA synthetase 3-mediated phosphatidylcholine synthesis is required for assembly of very low density lipoproteins in human hepatoma Huh7 cells. *J. Biol. Chem.* **283**, 849-854.

Genes to Cells

Tumor growth suppression *in vivo* by overexpression of the circadian component, PER2

Koyomi Miyazaki[1], Miyuki Wakabayashi[1], Yasuhiro Hara[1,2] and Norio Ishida[1,2]*

[1]*Clock Cell Biology Group, Institute for Biological Resource and Function, National Institute of Advanced Industrial Science and Technology (AIST), Tsukuba Central 6, 1-1-1, Higashi, Tsukuba, Ibaraki 305-8566, Japan*
[2]*School of Life and Environmental Sciences, University of Tsukuba, Tsukuba, Ibaraki, 305-8572, Japan*

Some reports have indicated that the core clock gene, *Per2* regulates the cell cycle, immune system and neural functions. To understand the effects of PER2 on tumor growth *in vivo*, stable transformants of murine sarcoma 180 (S-180) cell lines expressing different levels of PER2 were established. The growth of stable PER2 transformants *in vivo* was significantly and dose-dependently suppressed according to the amount of PER2 expressed, indicating that PER2 plays a role in the growth suppression of sarcoma cells. The anchorage-dependent and -independent growth *in vitro* and expression of the clock controlled cell-cycle related genes, *wee1*, *myc*, and *VEGF* were not altered in stable PER2 transformants. In contrast, susceptibility to murine natural killer (NK) cell cytolytic activity was enhanced in PER2 transformants. Furthermore, PER2 transformants suppressed cell motility and reduced fibronectin expression, but the expression of integrin receptors was not affected. These results suggest that sarcoma cells overexpressing PER2 suppress tumors *in vivo* by changing the nature of tumor cell adhesion.

Introduction

Most mammalian physiological, biochemical and behavioral processes oscillate daily with respect to time of day to adapt to daily environmental changes such as light, temperature and social communication. Circadian clock functions comprise transcription-translation feedback loops maintained by the core clock genes, *Clock, Bmal1, Period (Per*1, 2, 3) and *Cryptochrome (Cry1* and *Cry2*) (Reppert & Weaver 2001; Young & Kay 2001). Circadian clocks reside within all mammalian cells. Autonomous cellular rhythms in peripheral tissues such as the liver, heart and kidney are coordinated by signals from the suprachiasmatic nuclei (SCN) in the hypothalamus (Weaver 1998). Many genes are deregulated in the livers of mutant mice with dysfunctional clock genes (Oishi *et al.* 2003). Among such deregulated genes some, such as *wee1*, regulate the cell cycle, indicating that it is controlled by circadian clock molecules.

Recent molecular characterization of the mammalian oscillator has revealed that the circadian clock is involved in cellular pathways that are critical for cell division and tissue homeostasis. Levels of the checkpoint regulator for G2/M transition, *wee1*, are elevated and liver regeneration after partial hepatectomy is delayed in *Cry*-deficient mice compared with wild-type controls (Matsuo *et al.* 2003). Exogenously expressed *Per1* enhances apoptosis after irradiation through interacting with the checkpoint proteins ATM and Chk2 *in vitro* (Gery *et al.* 2006). CRY2 binds to the clock molecule, Timeless, and to the Chk1/ATR-ATRIP complex, and then regulates the DNA damage checkpoint response (Unsal-Kacmaz *et al.* 2005). Several lines of evidence generated from cancer studies indicate that PER2 also plays an important role in growth control and tumor development (Ishida 2007). In mice with a *Per2* mutation, *myc* transcription is up-regulated and protein induction of p53 after γ-radiation is downregulated, which consequently increases the incidence of tumors in these animals as well as the rate of mortality after exposure to ionizing radiation (Fu *et al.* 2002). The downregulation of *Per2* accelerates the growth of breast cancer by altering its daily growth rhythm (Yang *et al.* 2008). On the other hand, *Per2* overexpression in breast cancer cells leads to significant

Communicated by: Yoshiaki Ito
**Correspondence*: n.ishida@aist.go.jp

DOI: 10.1111/j.1365-2443.2010.01384.x

growth inhibition through estrogen receptor degradation *in vitro* (Gery *et al.* 2007). This finding suggests that PER2 also affects cancer cell growth through processes other than cell cycle regulation.

The circadian clock also controls tumor progression. Tumor growth is accelerated in mice with a lesioned SCN or in jet-lagged mice that have lost the 24-h rest/activity cycle (Filipski *et al.* 2002, 2004). In addition, PER2 modulates the expression of *VEGF*, which plays key roles in angiogenesis for tumor growth through antagonizing the formation of HIF-1α and ARNT complexes (Koyanagi *et al.* 2003). Circadian timing systems are disrupted in tumor cells *in vivo*, while rhythm generation in tumors recovers after the administration of an anti-tumor drug at a time that coincides with tumor growth suppression (Iurisci *et al.* 2006). These data suggest that regulation of the circadian system and tumor growth are closely related and that PER2 could be a good target for tumor suppression *in vivo* (Ishida 2007).

Here, we established sarcoma cell lines that stably overexpress PER2 and showed that PER2 transformants suppressed sarcoma growth in mice. However, the anchorage-dependent and independent cell growth of PER2 transformants *in vitro* and of parental sarcoma cells was similar. Transcriptional expression of the cell-cycle control genes, *wee1, myc, and VEGF,* was not significantly changed. As susceptibility to immune cells was enhanced and *fibronectin* transcription was suppressed by PER2 overexpression, we discuss a mechanism of tumor suppression through PER2 overexpression.

Results

Establishment of transformants overexpressing PER2 in tumor cells

Parental sarcoma 180 cells (S-180) normally produce minimal and barely detectable levels of *mPer2*. We established several cell lines that overexpress PER2 by transfecting hPER2 tagged with tandem affinity purification tag (TAP) expression cassettes into sarcoma 180 cells. Several transformants were selected and hPER2 protein expression levels were confirmed by Western blotting using an antibody against tagged Protein-A (Fig. 1a). Specific bands for exogenously expressed hPER2 were detected at various expression levels in the transformants but not in the parental sarcoma180 cells. The cell lines were classified according to the level of PER2 protein expression as hPER2-low, -medium1, -medium2 and high (-L, -M1, -M2, and –H, as shown in Fig. 1a, bottom). Quantitative RT-PCR analysis showed that transcription levels of exogenously expressed *hPer2* corresponded to expressed protein levels in stable transformants, but

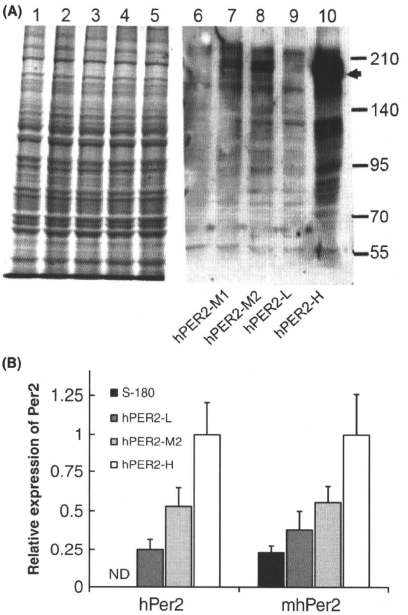

Figure 1 Establishment of sarcoma 180 stable transformant expressing hPER2. (a) Cell lysates were separated by SDS-PAGE and stained with Coomassie Brilliant Blue (lane 1–5). Expression of hPER2 was revealed by Western blotting using anti Protein-A antibody (arrow head in lane 6–10). Relative molecular weight sizes are shown on right. Compared with parental sarcoma 180 cells (lane 1 and 6), protein levels of exogenously expressed hPER2 are diverse among cell lines. Clones are named hPER2-L (lane 4 and 9), hPER2-M1 (lane 2 and 7), hPER2-M2 (lane 3 and 8), and hPER2-H (lane 5 and 10). (B) Expression levels of PER2 mRNA were semi-quantified by RT-PCR. Total RNA was extracted from sarcoma 180, hPER2-L, hPER2-M2 and hPER2-H, and mRNA levels of exogenous *hPer2* and total *Per2* (*mhPer2*; endogenous *mPer2* and exogenous *hPer2*) were measured by RT-PCR using respective specific primer sets. Maximal value for hPER2-H is expressed as 1. Values are means ± SEM (n = 4).

were detectable in S-180 cells (Fig. 1b). Furthermore, enhanced total *Per2* expression, which is the sum of endogenous *mPer2* and exogenous *hPer2* transcripts, was also confirmed in stable transformants, and the expression level of *Per2* in hPER2-H was almost five fold higher than that in S-180 cells (Fig. 1b). This indicated that exogenous *hPer2* expression overcomes endogenous *mPer2* expression in stable transformants.

Suppression of tumor growth by PER2 stable transformants *in vivo*

To determine whether PER2 overexpression affects the growth of tumor cells *in vivo*, we inoculated the hindlimb foot-pads of ICR mice with parental sarcoma180, hPER2-L, hPER2-M2, and hPER2-H and then measured the volume of each tumor three times each week for 3 weeks. Figure 2 shows significant increases in the tumor volume of S-180 and hPER2-L for up to 21 days after inoculation, while the growth of hPER2-M and hPER2-H was significantly suppressed ($P < 0.01$). Tumor growth of hPER2-H *in vivo* was more suppressed than that of hPER2-M, which was consistent with the PER2 expression level.

Cell growth of PER2 stable transformants *in vitro*

To determine whether PER2 affects antitumor activity *in vivo* due to cell growth suppression, we examined anchorage-dependent proliferation to determine the role of PER2 in cell growth *in vitro*. Figure 3 shows that anchorage-dependent proliferation did not change regardless of the protein level of PER2 expression, while all of the stable transformants suppressed growth *in vitro* a little compared with that of the parental sarcoma 180 cells ($P < 0.01$). We also assayed colony formation in soft agar to determine the nature of anchorage-independent growth. The colony forming efficiency of cells overexpressing PER2 was not significantly affected (Fig. S1a). These data indicated that PER2 overexpression does not influence the growth of stable transformants *in vitro*.

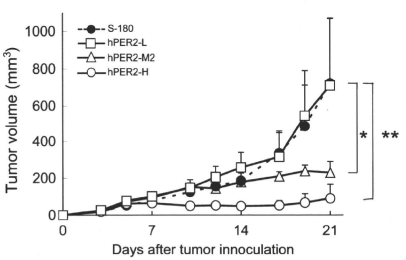

Figure 2 Tumor growth of PER2 stable transformants and parental sarcoma 180 cells in ICR mice. Sarcoma cell lines were inoculated subcutaneously into left hind footpads of ICR mice. Footpads were measured three times each week and plotted. (●) sarcoma 180, (□) hPER2-L, (△) hPER2-M2, (○) hPER2-H. Values are expressed as means ± SE ($n = 5$). Asterisks indicate that the differences in tumor volume are statistically significant between two values as indicated by lines (*$P < 0.01$, **$P < 0.001$ vs. hPER2-L).

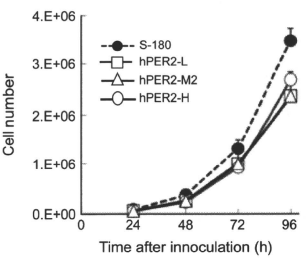

Figure 3 Growth rate of PER2 stable transformants *in vitro*. Cell lines (5×10^3) were inoculated into 35-mm plastic culture dishes and cells were counted 4 days later. (●) sarcoma 180, (□) hPER2-L, (△) hPER2-M2, (○) hPER2-H. Values from hPER2-L, hPER2-M2 and hPER2-H did not significantly differ.

Reports indicate that *Per2* modulates expression of the cell cycle regulators, *myc*, *wee1* and *VEGF* (Fu *et al.* 2002; Koyanagi *et al.* 2003; Matsuo *et al.* 2003). To understand the expression of these genes in PER2 transformants in sarcoma cells, we used quantitative RT-PCR to analyze their mRNA expression levels in lines stably expressing PER2. Figure S1b shows similar *myc*, *wee1* and *VEGF* expression among the stable PER2 lines. Furthermore, the amount of p53 protein, the transcription of which was upregulated during transient *Per2* expression in lung carcinoma cells (Hua *et al.* 2006), also did not differ in stable PER2 transformants (data not shown). These results are consistent with the absence of an effect on cell growth *in vitro* in the presence of stable PER2 expression. We speculate that PER2 overexpression in stable transformants plays a different role *in vivo* from cell growth control *in vitro*, resulting in tumor growth suppression.

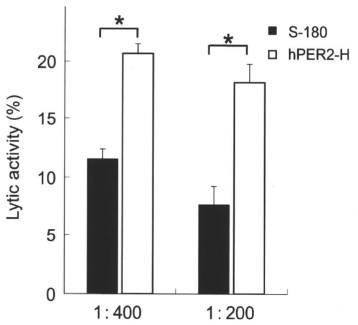

Figure 4 Cytolytic susceptibility of stable PER2 transformants to NK cells. Cytolytic activities of NK cells were calculated at 1 : 400 and 1 : 200 effector: target cell ratios in each experimental group. Values are expressed as means ± SE (n = 6). Shaded bar, parental sarcoma 180; solid bar, hPER2-H. Significant differences compared with values from sarcoma 180 and hPER2-H are indicated as $*P < 0.01$.

Enhanced susceptibility of cytolysis by NK cells in stable PER2 transformants

We examined that notion that the suppressive cell growth of PER2 transformants *in vivo* is due to clearance of transformants by the immune system. To directly examine the susceptibility of PER2 transformants to NK cytolytic attack, we measured the cytolytic activities of murine splenocyte CTL/NK cells against PER2 transformants as target cells. Figure 4 shows that effector cells had minimal or no cytolytic activity against parental sarcoma 180 cells, but significantly enhanced activity against hPER2-H (Fig. 4). This indicated that susceptibility to CTL/NK cells is accelerated in PER2 transformants.

Suppression of cell migration activity in stable PER2 transformants

Extracellular matrix on the surface of tumor cells can play important roles not only in cell migration but also in target recognition by the immune system. To determine whether PER2 overexpression affects cell migration activity, we examined the mobility of cell lines overexpressing PER2 by scratch tests. Confluent monolayers of parental sarcoma cells, hPER2-L, -M2, and –H were damaged by scratching with a tip and photographed immediately thereafter (0H) and at 3, 6, 9 and 12 h later. Motility was determined by measuring the remaining cleared distance and by calculating the distance migrated (Fig. 5a). The motility of cells overexpressing PER2 was dose-dependently suppressed, indicating that PER2 expression reduces cell migration.

Cell migration activity is mainly controlled by cell adhesion molecules, such as fibronectin, and their receptors (integrins). To test the effect of exogenously expressed PER2 on *fibronectin* and *integrin* expression, we compared the mRNA expression levels of these genes among stable transformants. Figure 5b shows that PER2 dose dependently suppressed *fibronectin*

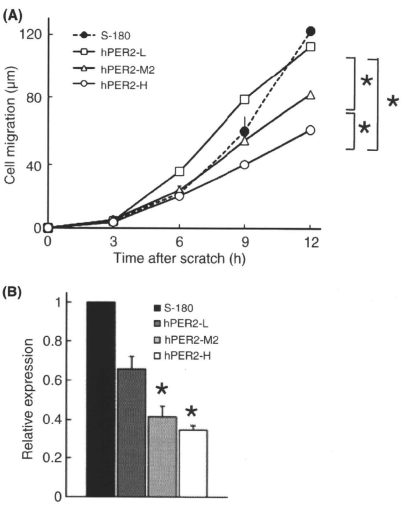

Figure 5 Stable PER2 overexpression suppresses cell migration. (a) Cell migration activity of PER2 stable transformants. Confluent monolayers of parental sarcoma 180 (●), hPER2-L (□), hPER2-M2 (△), and hPER2-H (○) were scratched with sterile pipette tips and cells were allowed to migrate into the wound for 3, 6, 9 and 12 h, before distance migrated was measured. Values are expressed as means ± SE (n = 6). Asterisks indicate statistically significant differences in migration between two values as indicated by lines ($*P < 0.001$). (b) RT-PCR analysis of *fibronectin* in PER2 stable transformants. Messenger RNA levels of *fibronectin* were normalized by comparison with β-*actin* mRNA expression and are shown as relative values to that expressed in parental cells. Values are expressed as means ± SE (n = 5). Asterisks indicate $P < 0.01$ vs. hPER2-L.

expression. On the other hand, expression levels of *integrins*, including *integrin* $\alpha 1$, $\alpha 5$, and $\beta 1$, did not significantly differ among stable transformants (Fig. S2). *Integrin* $\beta 3$ transcripts were detectable in mouse embryonic fibroblasts, but not in either parental sarcoma 180 cells or stable transformants (data not shown).

Discussion

Per2 plays roles not only in circadian rhythm generation but also in cell cycle regulation (Fu *et al.* 2002; Gery *et al.* 2007), and tumor development after γ-irradiation is obviously increased in mice deficient in the *mPer2* gene (Fu *et al.* 2002). These findings suggest that *Per2* plays a role in tumor suppression and that it can be used as cancer therapy after gene transfer. To understand whether exogenously transferred PER2 can suppress the growth of cancer, we established tumor cell lines that stably express PER2 and analyzed their growth *in vivo*. We selected the sarcoma 180 cell line as the parent of the stable lines, because it has been studied in detail from the viewpoint of transplantation and transient overexpression of *mPer2* suppresses *Vegf* expression (Koyanagi *et al.* 2003).

Overexpressed PER2 significantly and dose-dependently inhibited the subcutaneous growth of sarcoma 180 tumors. However, PER2 overexpression inhibited neither anchorage dependent- nor -independent growth of sarcoma cells *in vitro*, or the expression of the *myc, wee1, VEGF* genes that regulate the cell cycle. On the other hand, PER2 overexpression retarded cell migration activity and enhanced susceptibility to cytolytic attack by CLT/NK cells. We therefore concluded that the growth suppression of tumor cells expressing PER2 would be due to enhanced susceptibility to the immune system, and not to the control of cell growth.

Others have indicated that transient *Per2* overexpression can induce cell cycle arrest and apoptosis through alterations in apoptosis-related gene expression (Hua *et al.* 2006) in lung and breast carcinoma cells. In addition, *Per2* overexpression in breast carcinoma cells inhibits anchorage-independent growth through the estrogen receptor signaling pathway (Gery *et al.* 2007). However, the stable overexpression of *Per2* in sarcoma 180 cells did not alter either the growth rate *in vitro* or the expression of cell cycle-related genes in this study. This might be due to differences between sarcoma and carcinoma cell types. However, the possibility that the expression of other genes is altered cannot be excluded.

The expression of genes involved in cell cycle regulation and tumor suppression, such as *myc, cyclin D1, Mdm-2,* and *wee1* are deregulated in *mPer2* mutant, and in *clock* mutant mice. However, *myc* and *wee1* expression was not altered by PER2 overexpression in sarcoma 180 cells. The profiles of transcriptional oscillation of *Bmal1* and endogenous *mPer2* were similar both in stable PER2 transformants and in control sarcoma 180 cells after dexamethasone stimulation (Fig. S3). However, the amplitude of *Bmal 1* and endogenous *mPer2* expression was partially suppressed in hPER2-H. The oscillation of PER2 protein is maintained even in cells constitutively overexpressing the *Per2* gene because posttranslational modifications such as phosphorylation, degradation and nuclear-cytosol shuttling are mainly regulated to maintain circadian rhythms (Yamamoto *et al.* 2005). The circadian clock remained intact in sarcoma cells overexpressing PER2, and this is one explanation for why the expression of clock controlled genes that regulate the cell cycle or apoptosis was not altered. The anti-tumor effect of cells overexpressing PER2 *in vivo* cannot be explained simply by a change in the nature of cell growth *in vitro*.

Cell migration or metastasis is a crucial stage in tumor development *in vivo*. The overexpression of PER2 dose-dependently and significantly suppressed cell migratory activity *in vitro*. Furthermore, the expression of *fibronectin*, a major component of extracellular matrix, was reduced in cells expressing PER2, whereas *integrin* expression was not altered. Extracellular matrix and its integrin receptors contribute to cell proliferation and the migratory capacity of cells. Cell surface fibronectin was originally described as a protein that disappears upon transformation, whereas increased *fibronectin* expression enhances tumor malignancy in some cell lines (Hynes 1973; Akiyama *et al.* 1995; Akamatsu *et al.* 1996; Shimao *et al.* 1999; Beier *et al.* 2007). Partially suppressed fibronectin expression induces cellular detachment, which enables macrophages and T-lymphocytes to pass by (Beier *et al.* 2007). Our data suggested that the downregulation of *fibronectin* in sarcoma 180 cells overexpressing PER2 reduces their migratory activity and renders them vulnerable to attack by the CLT/NK immune systems.

Natural killer cells are innate lymphocytes that play important roles in immune defense against tumor cells. Natural killer cells are endowed with cell surface receptors that allow them to discriminate between normal and malignantly transformed cells. Beta 1 integrin is a key component in the NK cell recognition of target cells (Kuznetsov 1996). Thus, ligands

for integrin, such as fibronectin, laminin and VCAM, can antagonize binding between NK and target cells (Hiserodt *et al.* 1985; Kuznetsov 1996). The overexpression of PER2 might suppress *fibronectin* expression on tumor cells and thereby render them better targets for NK cells. If so, then the regression of stable PER2 transformant tumors *in vivo* might be due to clearance by the CLT/NK immune systems.

The expression of FN was inhibited in stable PER2 transformants. Precisely how overexpressed PER2 affects the gene expression of FN is unclear. Fibronectin gene expression is regulated through TGF-β signals (Hocevar *et al.* 1999) and the cAMP-dependent phosphorylation pathway (Dean *et al.* 1989). A key component of the cAMP-dependent phosphorylation pathway, CREB2, regulates *Per2* expression and *vice versa* in *Drosophila* (Belvin *et al.* 1999) and PER2 might affect the cAMP pathway through an unknown mechanism in mammals.

Several investigations including the present study indicate that *Per2* gene transfer improves tumor malignancy, even though the mechanisms of the tumor suppressive effects differed in every report. The overexpression of PER2 in sarcoma 180 cells inhibited tumor growth through affecting immune responsiveness, without changing circadian rhythm generation. Rhythmic expression of clock related genes is important for anti-tumor activity (Iurisci *et al.* 2006). The present study brings novel insight to the notion that the clock gene *Per2* could serve as a promising target for gene therapy of cancer.

Experimental procedures

Cell culture and isolation of stable transformants

Sarcoma 180 cells (Dainippon Pharmaceutical Co. Ltd.) were maintained in Dulbecco's modified Eagle's medium (DMEM) supplemented with 10% fetal calf serum and antibiotics (S-DMEM) under a 5% CO_2 atmosphere.

Human *Per2* cDNA (Gene bank no. NM_022817) was subcloned into the eukaryotic expression vector pcDNA 3 (Invitrogen). A tandem affinity purification (TAP) tag was cloned in-frame upstream of human *Per2* cDNA as described (Hara *et al.* 2009). A linearized expression plasmid cassette (3 μg) was transfected into 1×10^6 sarcoma 180 cells using Lipofectamine Plus (Invitrogen) according to the manufacturer's instructions and incubated in normal culture medium (S-DMEM) for 24 h. This medium was replaced with normal medium (S-DMEM) containing 500 μg/mL of G418 (Wako) and the cells were cultured for 4 days. Colonies exhibiting G418 resistance were harvested with 0.125% Trypsin/0.01% EDTA (Sigma), and then diluted to isolate single colonies for 2 weeks.

SDS-PAGE and Western blotting

Expression levels of human PER2 in stable transformants were analyzed by Western blotting. Harvested cells were rinsed with phosphate buffered saline (PBS) twice, lysed with lysis buffer (150 mM NaCl, 5 mM EDTA, 0.5% NP-40 and 50 mM Tris–HCl (pH 8.0)) including protease inhibitor cocktail tablets (Complete™; Roche) on ice for 30 min, then clarified by centrifugation for 10 min at 15 000 × *g*. Protein concentrations of cell lysates were determined using Protein Assays (BioRad) according to the manufacturer's instructions. Cell lysate proteins (150 μg) were boiled in sodium dodecyl sulfate (SDS) sample buffer, resolved by SDS-polyacrylamide gel electrophoresis (PAGE) and transferred onto nitrocellulose membranes (BioRad). Non-specific binding on the blots was blocked with 3% skim milk and then the blots were incubated with goat anti protein A antibody that recognizes a Protein A tag (Abcam) for 1 h at room temperature. After three rinses with 0.05% Tween 20 in PBS (T-PBS), proteins were detected using anti-goat IgG antibody conjugated with horseradish peroxidase (Santa Cruz) combined with enhanced chemiluminescence (GE Healthcare).

Animals

The Animal Care and Use Committee at AIST approved this study. ICR mice purchased from Japan SLC Co. (Hamamatsu, JAPAN) were synchronized to a 12-h light : 12-h dark cycle with food and water *ad libitum* for at least 2 weeks before starting experiments. Tumor cells (1.5×10^6 in 50 μL) were injected into the left hind footpads of each mouse. Tumor volume (mm^3) was calculated as XYZ, where X, Y, and Z are the perpendicular diameters of the tumor.

Anchorage-dependent and -independent cell growth

Cell growth and proliferation was assessed using cell growth curves and colony forming assays. Sarcoma 180 or PER2 stable transformants (2×10^5 cells) were seeded and cultured at 37 °C and then counted for 4 days using a hemocytometer and a microscope. Sarcoma 180 or PER2 stable transformants (5×10^3 cells/well) were seeded in 0.3% agarose (Sigma) supplemented with S-DMEM to examine anchorage-independent growth. Suspensions were layered over 0.7% agarose-medium base layers in 60-mm culture dishes (Nunc) and then colonies were counted under a microscope 15 days later.

Quantitative RT-PCR

Total cellular RNA isolated using the RNAiso reagent (TAKARA Bio Inc.) was treated with RNase-free DNaseI (TAKARA Bio Inc.) to eliminate contaminating genomic DNA, purified with RNAiso once again, and reverse transcribed (RT) using the PrimeScriptTM RT reagent kit

(TAKARA Bio Inc.) as described (Hara *et al.* 2009). Quantitative R.T polymerase chain reactions proceeded using SYBR® Premix Ex Taq™ (TAKARA Bio Inc.) and LightCycler™ (Roche). The primer sequences were: *hPer2*-for, GCGCTAA GGTCCAGTGATAAG; *hPer2*-rev, GGGCAGGCCCGCC AGGCAG; *mPer2*-for, AACTATCTCCAGGAGCGGTC; *mPer2*-rev, GTGTGGATACTATTCCGGGTGC; *mhPer2*-for, AAGGAGCTGAAGGTCCACCTCC; *mhPer2*-rev, GAGA TGTACAGGATCTTCCCAG; *myc*-for, CGTGACCAGATC CCTGA; *myc*-rev, TGCTCGTCTGCTTGAATG; *wee1*-for, CTGCTCCATTCCTCAGGAC; *wee1*-rev, TTGTTTCATC TTCAAACTCATAATCACT; *VEGF*-for, TCGTGGGAC TGGATTCG; *VEGF*-rev, ATGTGGGTGGGTGTGTCTA; *fibronectin*-for, GTGTGAGCGACATGCTCTA; *fibronectin*-rev, GTGACACAGTGGCCGTA; *integrin* $\alpha 1$-for, GCTATTCAG ATATCCAAAGACGG; *integrin*-$\alpha 1$-rev, TCCAATCTTCCA CAGAGCTAA; *integrin* $\alpha 5$-for, TGGCTATGTCACCGTCC TTA; *integrin* $\alpha 5$-rev, AGCCCATCTCCATTGGTA; *integrin* $\beta 1$-for, TTTGAAAAGGAGAAAATGAATGCCA; *integrin* $\beta 1$-rev, CATTTTCCCTCATACTTCGG; *integrin* $\beta 3$-for, GTGCTGACGCTAACCGA; *integrin* $\beta 3$-rev, CAGCCAAT TTTTTCATCACATAC; β-*actin*-for, CACACCTTCTACA ATGAGCTGC; β-*actin*-rev, CATGATCTGGGTCATCTTT TCA. Denaturation and amplification conditions were 95 °C for 10 s followed by 40 cycles of RT-PCR. Each cycle included 95 °C for 5 s, 57 °C for 10 s and 72 °C for 10 s for denaturation, primer annealing and extension/synthesis, respectively.

Natural killer (NK) cell cytotoxicity assay

Sarcoma 180 and stably transformed cells (2.5×10^3 cells) were seeded into 96 well plates (Nunc) and cultured overnight. The wells were rinsed with PBS and the medium was replaced with RPMI-1640 (Wako) supplemented with 1% FCS. Purified splenocytes prepared as described (Nishio *et al.* 2003) were added to each well as effector cells in a 200 : 1 or 400 : 1 ratio to target cells. After a 5-h incubation at 37 °C, 100 μL of supernatant was harvested and lactate dehydrogenase activity was determined using the LDH-Cytotoxic Test Wako (Wako) as cytolytic activity. The ratio (%) cytotoxicity is expressed as follows: % cytotoxicity = (OD of experimental well-OD of effector spontaneous-OD of target spontaneous)/OD of target maximum release in control well) × 100.

Cell migration assay

Confluent cell monolayers in tissue culture dishes were wounded by scratching with a pipette tip, washed with PBS and incubated at 37 °C in S-DMEM to analyze cell migration. Phase-contrast images at specific wound sites were captured at 0, 3, 6, 9 and 12 h later. Numbers of pixels between the edges of cell layers were calculated using Adobe Photoshop (Adobe Systems, San Jose, CA, USA). Three independent experiments were averaged and the SEMs of the final time point are represented.

Statistical analysis

The results are expressed as mean values ± SEM. The statistical significance of differences between results was evaluated using one-way or two-way ANOVA and *P*-values were calculated. A value of $P < 0.05$ was accepted as statically significant.

Acknowledgements

This study was supported by an AIST internal grant. We thank K. Oishi, Y. Miyamoto, and T. Okada for helpful discussion, K. Suzuki for excellent technical assistance and I. Shibasaki and H. Tanaka for maintaining the mice.

References

Akamatsu, H., Ichihara-Tanaka, K., Ozono, K., Kamiike, W., Matsuda, H. & Sekiguchi, K. (1996) Suppression of transformed phenotypes of human fibrosarcoma cells by overexpression of recombinant fibronectin. *Cancer Res.* **56**, 4541–4546.

Akiyama, S.K., Olden, K. & Yamada, K.M. (1995) Fibronectin and integrins in invasion and metastasis. *Cancer Metastasis Rev.* **14**, 173–189.

Beier, U.H., Holtmeier, C., Weise, J.B. & Gorogh, T. (2007) Fibronectin suppression in head and neck cancers, inflammatory tissues and the molecular mechanisms potentially involved. *Int. J. Oncol.* **30**, 621–629.

Belvin, M.P., Zhou, H. & Yin, J.C. (1999) The Drosophila dCREB2 gene affects the circadian clock. *Neuron* **22**, 777–787.

Dean, D.C., Blakeley, M.S., Newby, R.F., Ghazal, P., Hennighausen, L. & Bourgeois, S. (1989) Forskolin inducibility and tissue-specific expression of the fibronectin promoter. *Mol. Cell. Biol.* **9**, 1498–1506.

Filipski, E., Delaunay, F., King, V.M., Wu, M.W., Claustrat, B., Grechez-Cassiau, A., Guettier, C., Hastings, M.H. & Francis, L. (2004) Effects of chronic jet lag on tumor progression in mice. *Cancer Res.* **64**, 7879–7885.

Filipski, E., King, V.M., Li, X., Granda, T.G., Mormont, M.C., Liu, X., Claustrat, B., Hastings, M.H. & Levi, F. (2002) Host circadian clock as a control point in tumor progression. *J. Natl Cancer Inst.* **94**, 690–697.

Fu, L., Pelicano, H., Liu, J., Huang, P. & Lee, C. (2002) The circadian gene Period2 plays an important role in tumor suppression and DNA damage response in vivo. *Cell* **111**, 41–50.

Gery, S., Komatsu, N., Baldjyan, L., Yu, A., Koo, D. & Koeffler, H.P. (2006) The circadian gene per1 plays an important role in cell growth and DNA damage control in human cancer cells. *Mol. Cell* **22**, 375–382.

Gery, S., Virk, R.K., Chumakov, K., Yu, A. & Koeffler, H.P. (2007) The clock gene Per2 links the circadian system to the estrogen receptor. *Oncogene* **26**, 7916–7920.

Hara, Y., Onishi, Y., Oishi, K., Miyazaki, K., Fukamizu, A. & Ishida, N. (2009) Molecular characterization of Mybbp1a

as a co-repressor on the Period2 promoter. *Nucleic Acids Res.* **37**, 1115–1126.

Hiserodt, J.C., Laybourn, K.A. & Varani, J. (1985) Laminin inhibits the recognition of tumor target cells by murine natural killer (NK) and natural cytotoxic (NC) lymphocytes. *Am. J. Pathol.* **121**, 148–155.

Hocevar, B.A., Brown, T.L. & Howe, P.H. (1999) TGF-beta induces fibronectin synthesis through a c-Jun N-terminal kinase-dependent, Smad4-independent pathway. *EMBO J.* **18**, 1345–1356.

Hua, H., Wang, Y., Wan, C., Liu, Y., Zhu, B., Yang, C., Wang, X., Wang, Z., Cornelissen-Guillaume, G. & Halberg, F. (2006) Circadian gene mPer2 overexpression induces cancer cell apoptosis. *Cancer Sci.* **97**, 589–596.

Hynes, R.O. (1973) Alteration of cell-surface proteins by viral transformation and by proteolysis. *Proc. Natl Acad. Sci. USA* **70**, 3170–3174.

Ishida, N. (2007) Circadian clock, cancer and lipid metabolism. *Neurosci. Res.* **57**, 483–490.

Iurisci, I., Filipski, E., Reinhardt, J., Bach, S., Gianella-Borradori, A., Iacobelli, S., Meijer, L. & Levi, F. (2006) Improved tumor control through circadian clock induction by Seliciclib, a cyclin-dependent kinase inhibitor. *Cancer Res.* **66**, 10720–10728.

Koyanagi, S., Kuramoto, Y., Nakagawa, H., Aramaki, H., Ohdo, S., Soeda, S. & Shimeno, H. (2003) A molecular mechanism regulating circadian expression of vascular endothelial growth factor in tumor cells. *Cancer Res.* **63**, 7277–7283.

Kuznetsov, V.A. (1996) "Harpoon" model for cell-cell adhesion and recognition of target cells by the natural killer cells. *J. Theor. Biol.* **180**, 321–342.

Matsuo, T., Yamaguchi, S., Mitsui, S., Emi, A., Shimoda, F. & Okamura, H. (2003) Control mechanism of the circadian clock for timing of cell division in vivo. *Science* **302**, 255–259.

Nishio, N., Oishi, K. & Machida, K. (2003) SST-2 tumor inoculation is a useful model for studying the anti-tumor immune response in SHR rat. *Environ. Health Prev. Med.* **8**, 1–5.

Oishi, K., Miyazaki, K., Kadota, K., *et al.* (2003) Genome-wide expression analysis of mouse liver reveals CLOCK-regulated circadian output genes. *J. Biol. Chem.* **278**, 41519–41527.

Reppert, S.M. & Weaver, D.R. (2001) Molecular analysis of mammalian circadian rhythms. *Annu. Rev. Physiol.* **63**, 647–676.

Shimao, Y., Nabeshima, K., Inoue, T. & Koono, M. (1999) Role of fibroblasts in HGF/SF-induced cohort migration of human colorectal carcinoma cells: fibroblasts stimulate migration associated with increased fibronectin production via upregulated TGF-beta1. *Int. J. Cancer* **82**, 449–458.

Unsal-Kacmaz, K., Mullen, T.E., Kaufmann, W.K. & Sancar, A. (2005) Coupling of human circadian and cell cycles by the timeless protein. *Mol. Cell. Biol.* **25**, 3109–3116.

Weaver, D.R. (1998) The suprachiasmatic nucleus: a 25-year retrospective. *J. Biol. Rhythms* **13**, 100–112.

Yamamoto, Y., Yagita, K. & Okamura, H. (2005) Role of cyclic mPer2 expression in the mammalian cellular clock. *Mol. Cell. Biol.* **25**, 1912–1921.

Yang, X., Wood, P.A., Oh, E.Y., Du-Quiton, J., Ansell, C.M. & Hrushesky, W.J. (2009) Down regulation of circadian clock gene Period 2 accelerates breast cancer growth by altering its daily growth rhythm. *Breast Cancer Res. Treat.* **117**, 423–431.

Young, M.W. & Kay, S.A. (2001) Time zones: a comparative genetics of circadian clocks. *Nat. Rev. Genet.* **2**, 702–715.

Received: 21 June 2009
Accepted: 30 December 2009

Supporting Information/Supplementary Material

The following Supporting Information can be found in the online version of the article:

Figure S1 (a) Colony formation assay of parental sarcoma 180 and PER2 stable transformant lines. Cell lines were embedded into soft agar and colonies were counted 15 days later. Colony formation is expressed as number of colonies divided by number of inoculated cells. Values are expressed as means ± SE (n = 5). (b) RT-PCR analysis of cell cycle regulated genes, *myc, wee1* and *VEGF* in stable PER2 transformants. Messenger RNA levels of each gene were normalized by comparison with *β-actin* mRNA expression and are shown as relative values to expression in parental cells. Values are expressed as means ± SE (n = 4).

Figure S2 RT-PCR analysis of *integrins α1, α5, and β1* in stable PER2 transformants. Messenger RNA levels of each gene were normalized by comparison with mRNA expression of *β-actin* and are shown as relative values to expression in parental cells. Values are expressed as means ± SE (n = 4).

Figure S3 Circadian expression profile of *Bmal1* (a) and endogenous *mPer2* (b) in sarcoma 180 (●) and hPER2-H (○). Dexamethasone (100 nM final concentration) was added to culture medium at time 0. Cells were collected at indicated time points and relative mRNA levels of clock genes were determined by RT-PCR. Value at time 0 was set to 1.

Additional Supporting Information may be found in the online version of this article.

Please note: Wiley-Blackwell are not responsible for the content or functionality of any supporting materials supplied by the authors. Any queries (other than missing material) should be directed to the corresponding author for the article.

The FASEB Journal • Research Communication

Oocyte-type linker histone B4 is required for transdifferentiation of somatic cells *in vivo*

Nobuyasu Maki,*,†,[1] Rinako Suetsugu-Maki,* Shozo Sano,† Kenta Nakamura,* Osamu Nishimura,‡ Hiroshi Tarui,† Katia Del Rio-Tsonis,§ Keita Ohsumi,¶ Kiyokazu Agata,†,‡ and Panagiotis A. Tsonis*,[1]

*Department of Biology and Center for Tissue Regeneration and Engineering at Dayton, University of Dayton, Dayton, Ohio, USA; †RIKEN Center for Developmental Biology, Kobe, Japan; ‡Department of Biophysics, Kyoto University, Kyoto, Japan; §Department of Zoology, Miami University, Oxford, Ohio, USA; and ¶Division of Biological Science, Nagoya University, Nagoya, Japan

ABSTRACT **The ability to reprogram *in vivo* a somatic cell after differentiation is quite limited. One of the most impressive examples of such a process is transdifferentiation of pigmented epithelial cells (PECs) to lens cells during lens regeneration in newts. However, very little is known of the molecular events that allow newt cells to transdifferentiate. Histone B4 is an oocyte-type linker histone that replaces the somatic-type linker histone H1 during reprogramming mediated by somatic cell nuclear transfer (SCNT). We found that B4 is expressed and required during transdifferentiation of PECs. Knocking down of B4 decreased proliferation and increased apoptosis, which resulted in considerable smaller lens. Furthermore, B4 knockdown altered gene expression of key genes of lens differentiation and nearly abolished expression of γ-*crystallin*. These data are the first to show expression of oocyte-type linker histone in somatic cells and its requirement in newt lens transdifferentiation and suggest that transdifferentiation in newts might share common strategies with reprogramming after SCNT.—Maki, N., Suetsugu-Maki, R., Sano, S., Nakamura, K., Nishimura, O., Tarui, H., Del Rio-Tsonis, K., Ohsumi, K., Agata, K., Tsonis, P. A. Oocyte-type linker histone B4 is required for transdifferentiation of somatic cells *in vivo*. *FASEB J.* 24, 3462–3467 (2010). www.fasebj.org**

Key Words: newt · lens regeneration · histone H1 · γ-crystallin

As stem or progenitor cells are diverted to differentiate toward a particular lineage, they lose their multipotentiality. At the endpoint, when they are terminally differentiated, cells are thought to be unable to revert to multipotent state. Contrary to this finding, the case of newt lens regeneration is a prime paradigm of transdifferentiation at work. After lens removal, the iris pigmented epithelial cells (PECs) dedifferentiate and then change their fate to become lens cells. Four to 5 d after lentectomy, the pigmented cells at the tip of the dorsal iris shed their pigments and start proliferating, thus losing their original tissue characteristics. Depigmented cells are observed initially around d 8. At 13 or 14 d after lentectomy, these depigmented PECs have formed a vesicle, which is still undifferentiated and expresses no lens-specific markers. The last step marks the onset of transdifferentiation and the formation of the lost lens. After d 14, the posterior cells of the vesicle elongate and start expressing lens markers. The vesicle grows and differentiates to lens, which by d 20 has a considerable size and normal morphology. It is important to state here that while the ventral iris PECs undergo some of the initial events, they fail to transdifferentiate to lens. Transdifferentiation of PECs has been directly demonstrated by clonal culture experiments (1, 2).

Since transdifferentiation should involve large-scale reprogramming, we hypothesized that histones, which are known to regulate gene expression and reprogramming (3, 4), would be good candidates to explore such possibility. In this study, we focused on linker histones. Four types of linker histone, *i.e.*, somatic-, oocyte-, testis-, and erythrocyte-type linker histones, have been identified (5, 6). Oocyte-type linker histone, which is known to be expressed during oogenesis and early embryogenesis (7–12), is believed to play an important role in the reprogramming mediated by SCNT into oocyte. After SCNT somatic-type linker histone H1 is replaced by oocyte-type linker histone (13–15), which allows chromatin to be remodeled by an ATP-dependent chromatin remodeling factor (16) and causes genome-wide chromatin decondensation (17). Here we show that oocyte-type linker histone B4 is recruited specifically into nucleus and is necessary for lens transdifferentiation.

[1] Correspondence: University of Dayton, Department of Biology, 300 College Park, SC46, Dayton, OH 45469-2320, USA. E-mail: N.M., makinobu@notes.udayton.edu; P.A.T., panagiotis.tsonis@notes.udayton.edu

doi: 10.1096/fj.10-159285

0892-6638/10/0024-3462 © FASEB